J Mater Sci (2021) 56:999–1038

Review

Refinement of primary carbides in hypereutectic high-chromium cast irons: a review

Abhi-Shek Jain[1], Haiwei Chang[1], Xinhu Tang[1,2,*], Brook Hinckley[2], and Ming-Xing Zhang[1,*]

[1] School of Mechanical and Mining Engineering, University of Queensland, Brisbane, QLD 4072, Australia
[2] Weir Minerals Australia Ltd, Artarmon, NSW 2064, Australia

Received: 27 May 2020
Accepted: 19 August 2020
Published online: 23 September 2020

ABSTRACT

As a category of crucial wear-resistant alloys, high-chromium cast irons (HCCIs) are widely used in mining, minerals and cementation industries. The large volume fraction of coarse primary M_7C_3 carbides (PC) imparts excellent wear resistance. However, coarse carbides also induce brittleness, resulting in high cracking susceptibility, and early failure of components, particularly under impact. To minimize the brittleness and increase the service life of HCCI parts, different techniques have been developed through modifying the carbide morphology and refining its size. This paper comprehensively reviews the currently available methods that have either been used in industry production or in laboratory development to modify the primary M_7C_3 carbides in various HCCIs. The possible mechanisms that govern the refinement of primary carbides are also discussed in-depth. Based on previously published work, the mechanical performance of HCCIs is correlated with the microstructure of the matrix, and with the size, shape, volume fraction and distribution of primary carbides. This may provide solid fundamental to develop more effective techniques and/or new alloys to further improve the properties of this type of materials, increasing their engineering service life and to tailor their wider applications. In addition, the present work also seeks theoretical feasibility to apply the recently well-established theories/models of grain refinement for cast metals to refinement of the primary carbides in HCCIs.

Handling Editor: P. Nash.

Address correspondence to E-mail: tiger.tang@mail.weir; mingxing.zhang@uq.edu.au

https://doi.org/10.1007/s10853-020-05260-8

Introduction

On solidification of cast irons containing over 2 wt.% carbon and other alloying elements, carbide rather than graphite, forms, which enables a silver colour (white) fracture surface, and the alloy is named as "white" cast iron [1, 2]. Formation of such carbide results in the high hardness and superior wear resistance of this type of materials. The volume fraction, type and morphology of the carbide rely on the carbon content and the alloying elements contained in it. In case of hypoeutectic cast irons (the carbon content is below the eutectic point, ~ 2.5–4.1 wt.%), majority of the carbide is eutectic carbide in lamellar morphology. In hypereutectic cast irons, both Widmanstätten primary carbide and eutectic carbide form. Addition of chromium greater than 12 wt.% forms high-chromium cast irons [3]. It is known that the high chromium not only leads to improved corrosion resistance due to the generation of chromium oxide film on the surface [4], but also results in the formation of coarse hexagonal M_7C_3 carbides during solidification [5]. In addition, depending on the composition of the alloy and the heat treatment condition, the carbide in high-chromium cast irons (HCCI) can be $M_{23}C_6$, M_7C_3 or M_3C type of carbides [6, 7].

The presence of primary and eutectic M_7C_3 carbides with either austenitic matrix in as-cast condition or martensitic matrix in heat-treated condition gives rise to high hardness and excellent wear resistance [8]. Thus, high-chromium cast iron has found itself being used in multiple industries. From crushing equipment used in limestone and coal mines to being used as body, impellers, cover and back liners in slurry pumps. From being used as wear plates in conveyors handling abrasive material to being used as tiles in the furnace lining of blast furnace [9]. The highly alloyed white cast iron, first patented in 1917, was less brittle, very hard with excellent corrosion resistance as compared to unalloyed white irons [10]. From 1920, the Electro Metallurgical Company developed and used alloys with 15–35% chromium and 1.5–3% carbon in order to reduce maintenance of grinding and crushing equipment and in high-temperature applications [2]. Then, it was understood that the properties of HCCIs depend on the chromium carbides and the matrix. In 1962, Bradley and Foster, Ltd., examined the effects of alloy additions and heat treatment on the service life of the HCCIs with various chromium and carbon contents. This study led to castings that were free of pearlite and ferrite and had consistent abrasion resistance in as-cast condition [2]. Since then, most research is focussed on improving the abrasion resistance by either alloying additions or strengthening the matrix by destabilizing it [2].

In order to achieve higher performance, much higher chromium content was added in the HCCIs. However, the increase in proportion of carbides also leads to deterioration of fracture toughness of the material [11]. The primary and eutectic M_7C_3 carbides grow as rods and blades, respectively, in the longitudinal sections and as rods in the transverse section along the preferred growth axis [12–14]. Properties, such as abrasion resistance and fracture toughness, not only depend on carbide and matrix but also on the size, distribution, inter-carbide spacing, orientation, morphology and shape of the carbides [15–17]. Hence, controlling the carbide in HCCIs is very critical and necessary to achieve the desired properties.

Importance in modification of morphology of primary carbides in cast irons

Like all metallic materials, mechanical properties of HCCI are defined by its microstructure that consists of carbide and matrix. Depending on the heat treatment process, the matrix can be austenite and/or martensite and/or bainite. In hypoeutectic HCCI, the primary phase is austenite, which may transfer to martensite and/or bainite/pearlite during subsequent cooling or heat treatment. The eutectic carbide is generally finer. Thus, the cast iron has a good combination of hardness and toughness [18–20]. In contrast, hypereutectic HCCI has a large amount of coarse primary M_7C_3 carbides in the microstructure, resulting in high hardness and brittleness. For a particular composition, the carbide volume fraction (CVF) can be estimated using the Maratray's equation (Eq. 1 as follows) [21]. A deviation of 2–3% was found in the results calculated using the formula due to inclusion of eutectic and secondary carbides. The CVF can also be experimentally determined using wet chemistry [22, 23] and image analysis. The calculated result should ideally be similar to the experimentally determined result. However, as the

primary carbides become coarser, large standard deviation in CVF obtained from image analysis is generated due to variation in the number of carbide particles examined in images obtained at same resolution [24].

$$\begin{aligned} \mathrm{CVF}\% &= 12.33 \times (\%\mathrm{C}) + 0.55 \times (\%\mathrm{Cr}) - 15.2 \\ &= \pm 2.1\%\mathrm{CVF} \end{aligned} \quad (1)$$

The primary M_7C_3 carbides in hypereutectic HCCIs commonly appear as Widmanstätten structure and cannot be modified during subsequent heat treatment. Although such hard phase significantly contributes to the hardness and wear resistance of the alloy, it is brittle in nature and provides fast path for propagation of cracks [25]. Coronado [13] examined the effect of orientation of primary carbides and found that crack initiation and propagation occurred more easily along the larger edge of the carbides than perpendicular to it. Hebbar and Seshan [26] found increase in the amount of carbides on the fractured surface of a HCCI, suggesting pronounced cleavage fracture through the carbides or carbide–matrix interface. Adler and Dogan [27, 28] and Magnée [29] observed the fast and easy crack propagation in coarse primary carbides under impact leading to decrease in toughness and increase in erosion rate [30]. Hence, in order to minimize the cracking and increase the toughness of HCCIs, it is necessary and crucial to control the morphology of the primary carbides. Studies have shown that the properties of hypereutectic HCCIs were enhanced by proper alloys design and microstructure control [3, 6, 16, 31, 32]. Equiaxed primary M_7C_3 carbides have been verified to improve the toughness and wear resistance of HCCIs [33, 34]. Hence, in the past decades, considerable efforts have been made to modify the primary carbide in various HCCIs and a number of techniques have been developed.

Modification of primary carbides in high-chromium cast irons through process control

In hypereutectic HCCIs, primary carbides form directly from liquid in between the liquidus and eutectic temperature. Its volume fraction, size and morphology are governed by the carbon content, solidification process, cooling rate in particular, and carbide modifiers. Hence, process control and modification treatment are two common approaches to control the primary carbides. In this section, the currently available process control techniques are reviewed.

Control of casting process

The as-cast microstructure of HCCIs, particularly the size and distribution of the primary carbide, significantly varies with casting parameters, such as cooling rate and pouring temperature [8, 35]. Previous research indicated that the segregation of alloying elements is directly related to the cooling rate [36]. The amount of segregation of a particular alloying element in the microstructure is denoted by the Segregation Ratio (SR). It is the ratio of concentration of alloying element in the carbide to that in the matrix [37]. A high SR value for elements, such as carbon and chromium, indicates their strong presence in the carbides, while a low SR value for elements, such as nickel, silicon and copper, suggests that they are more likely to be found in the matrix [8, 38]. Yang et al. [39] and Yang and Lei [40] observed that SR for carbon is higher at high cooling rates, but there is no significant variation in chromium segregation with cooling rate. Higher cooling rates correspond to bigger undercooling, enhancing the nucleation of carbides, but also suppressing their growth due to the lower atomic diffusivity at lower temperature [41]. Thus, in the case of non-uniform cooling rate during casting, coarsening of primary carbides occurs in the regions with lower cooling rate [39]. Liu et al. [42] examined the effect of cooling rate by changing the mould from sand mould with slow cooling rate to metal mould with fast cooling rate. They observed a reduction in size of the primary carbides from 151.9 μm in sand mould to 53.9 μm as shown in Fig. 1. The refinement of primary carbides was attributed to the higher nucleation rate and relatively slower growth rate of the primary carbide due to the bigger thermal undercooling associated with the increase in cooling rate. Bigger undercooling thermodynamically provides higher solidification driving force, which promotes the nucleation of primary carbide. Furthermore, bigger undercooling also enables the slow growth of carbide as it occurs at lower temperatures. Hence, fine primary carbide forms at fast cooling during solidification of the HCCI. Variation in cooling rate does seem that

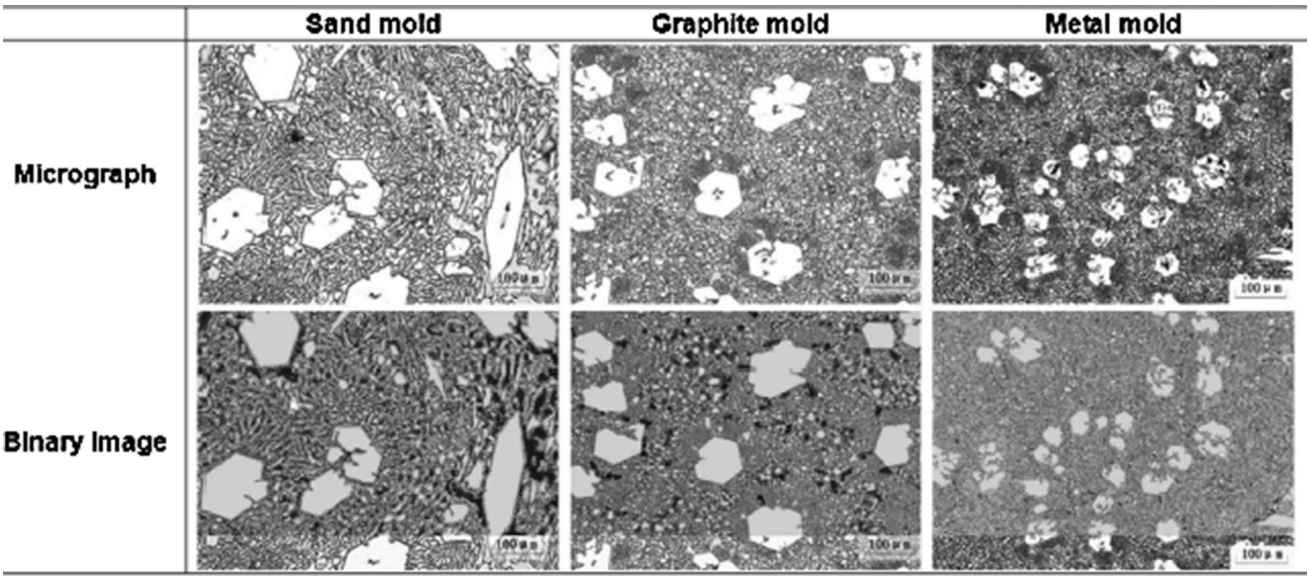

Figure 1 Micrographs of the as-cast Fe-16.2Cr-4.01C HCCI cast in sand mould, graphite mould and metal mould respectively. Adapted with permission from reference [42]. Copyright 2012, The Iron and Steel Institute of Japan.

increasing solidification rate is effective in refining the primary carbide in hypereutectic HCCIs. However, in industrial production, the large components are usually produced by sand casting. This implies that increase in cooling rate is very limited. In addition, in most cases, increasing cooling rate might not be practical because of the variation in cooling rates from the surface to the centre of large castings. For example, in a Fe-27.5Cr-2.87C cast iron, the size of primary carbide varied from very fine carbide with an average size of 1.54 μm at the surface formed at high cooling rate as shown in Fig. 2c to the coarse carbide with an average size of up to 5.2 μm at the centre formed at low cooling rate as shown in Fig. 2a [40]. Consequently, a decrease in carbide spacing and an increase in the number of carbide particles in regions with high cooling rate were also observed. This variation in the size and spacing of the primary carbide led to higher hardness and higher wear resistance in the chilled zone than in regions near the centre of the casting with relatively lower cooling rate. As a result, the variation of cooling rate from centre to surface led to high non-uniformity in mechanical properties [40, 43], which is not accepted for industry applications.

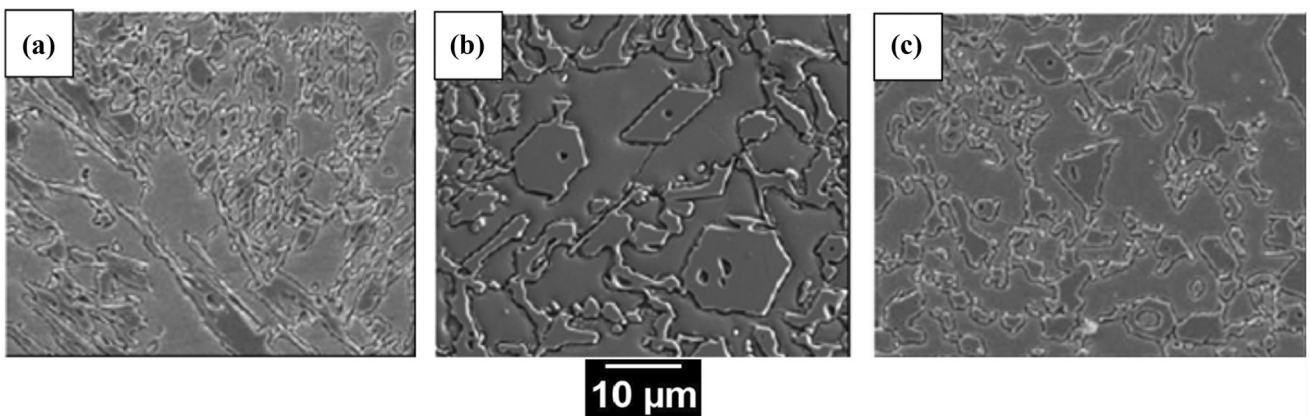

Figure 2 SEM micrographs of the Fe-27.5Cr-2.87C HCCI at the **a** centre of casting (low cooling rate), **b** mid-way between centre and wall of the casting (intermediate cooling rate) and **c** wall of the casting (high cooling rate). Adapted with permission from reference [40]. Copyright 2012, Taylor & Francis.

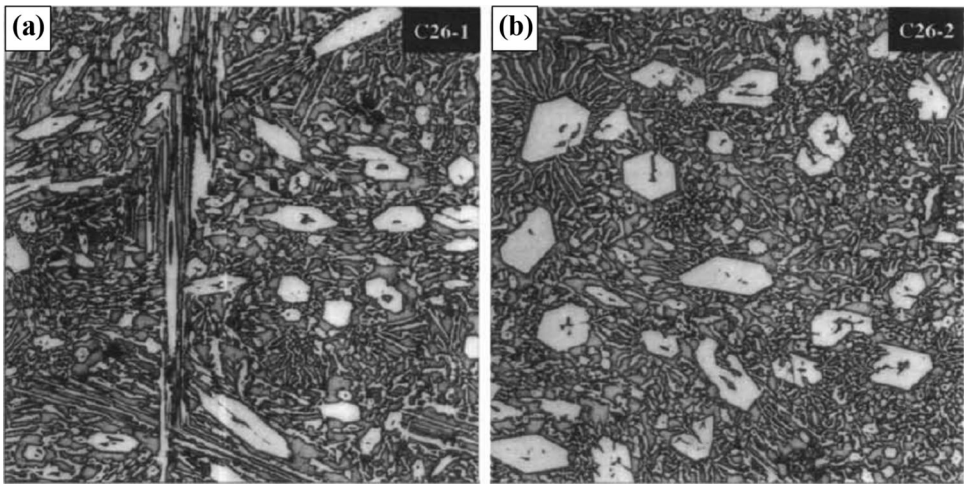

Figure 3 Optical micrographs of hypereutectic cast iron containing 26% Cr. **a** cast at low pouring temperature (50 °C above liquidus); **b** cast at high pouring temperature (250 °C above liquidus). Etched with Vilella's reagent. Adapted with permission from reference [43]. Copyright 1996, Taylor & Francis.

Pouring temperature is another casting parameter that significantly affects the size and distribution of primary carbides. Pouring at temperatures much above the liquidus of alloys results in coarsening of the primary carbides as shown in Fig. 3b [43]. This is because the high superheating heats up the cold mould, leading to lower cooling and solidification rates. Thus, primary carbide forms at relatively higher temperature, at which Cr and C atoms diffuse faster, promoting the growth of carbide. In addition, high pouring temperature corresponds to small thermal undercooling, and therefore low nucleation rate of the primary carbide. Even the formed nuclei are not stable and could be re-melted owing to the higher temperature [24]. This allows the growth of the M_7C_3 carbide along the preferred direction, leading to the formation of coarse prismatic needle-shaped carbide. When the pouring temperature is very close to the liquidus temperature, higher cooling and solidification rate is achieved, resulting in refinement of the primary carbides as shown in Fig. 3a. In addition, pouring at lower temperature is also related to smaller thermal gradient. Thus, the solidified primary carbides are fine, equiaxed and well distributed. The variation in morphology is due to change in pouring temperature, leading to variation in mechanical properties of HCCIs. Laird and Dogan [43] checked the hardness and impact toughness from the surface to the centre of a HCCI casting. They found that the hardness was significantly higher at the surface than that at the centre of the casting. This was attributed to the faster cooling on the surface of the casting, leading to the formation of very fine carbide particles. Obviously, the measured hardness on the surface cannot be regarded as the hardness of the HCCI casting due to the microstructural and hardness inhomogeneity. Furthermore, the impact toughness of the casting is directly influenced by the carbide size and its structure (columnar or equiaxed). Huang et al. [44] examined the effect of pouring temperature on the solidification of the Fe-17.10Cr-4.08C alloy via slope cooling body method by applying superheating of 17 °C, 37 °C and 57 °C. They reported that pouring with lowest superheating led to decrease in the size of primary carbides along with an increase in the number of shrinkage porosities in the microstructure, hence lowering the toughness of the alloy. This result contradicts the conclusion that finer primary carbide corresponds to higher toughness [27, 28]. The present authors consider that the shrinkage porosities on the surface were probably responsible for the lowering of toughness, which covered the positive effect of carbide refinement on the property. In addition, selection of proper pouring temperature also depends on external additions to the molten alloy and the composition of the alloy [41]. Hence, lowering the pouring temperature to refine the primary carbide of the HCCIs seems very limited.

Overall, high cooling rate leads to increase in the nucleation rate of primary carbide owing to the large undercooling, and lowering the growth rate as it occurs at lower temperatures [40, 42, 45]. Hence, finer carbide can be obtained. Similarly, lower pouring temperature implies less superheat, which is associated with higher cooling rate. As a result, primary carbide can also be refined through reduction in pouring temperatures [43].

Electric current pulse method

In addition to controlling the casting parameters, employing external interference is another effective approach to modify the morphology of primary carbide in hypereutectic HCCIs. A typical example is the electric current pulse (ECP) technique. Many researchers have worked on ECP to understand the mechanism by which it causes grain refinement in both ferrous and non-ferrous alloys [46–51]. In terms of the temperature the ECP is applied, the theory can be categorized into two classes. The first is to apply the ECP directly to the melt before the beginning of solidification. It is based on the theory of inoculation which states that when the electric pulse is passed through the melt, the bigger clusters break away while the small clusters polarize, causing strong electric field around it. Thus, the solute and the solvent atoms can surround and reorganize around the cluster, acting as inoculants, leading to nucleation [52–54]. The second involves applying the ECP during solidification. It is based on two major hypotheses [55–57]. One is the breaking of dendrites, which suggests that when ECP is passed through the casting, shear stress acts on the dendrites, breaking the fragmentation into globular particles that act as nucleants, leading to a refined microstructure [57, 58]. Another considers that the electric pulse causes compositional changes in the melt, leading to refinement of microstructure, due to the difference in ionic mobility [55, 56]. However, both these hypotheses still lack of solid experimental evidences to support. This may need in-depth study.

Chen et al. [46] applied ECP technique on a Fe-22.41Cr-4.2C HCCI at two pouring temperatures, 1350 °C and 1360 °C during solidification. The hypereutectic HCCI was first cast into sample sticks, which were then sealed with silica sand to avoid oxidation and put in a ceramic tube with electrodes connected to the sample. The tube with the sample stick in side was heated to desired temperatures. The ECP was applied during solidification at the temperature of 1350 °C and 1360 °C, respectively. The effect of ECP at different processing times and pouring temperature was investigated, and the results are illustrated in Fig. 4. Noticeable carbide refinement can be observed with increase in ECP treatment time up to 2.5 to 3.5 min, which were optimal ECP treatment times for the 1350 °C and 1360 °C pouring temperatures, respectively [46]. Further increasing the ECP time led to coarsening of the carbide. Lv et. al. applied the ECP when the melt was in a temperature range from 1360 °C to 1276 °C. A decrease in the average diameter of the primary carbides from 220 μm to 60 μm was found. They also reported the change in morphology of primary carbides from thick long rods to hexagonal granular or block structures [51].Chen et al. [46] attributed the refinement of carbides to the ECP induced periodic Lorenz force that led to an additional convection to the melt. Under this Lorenz force, fine nuclei particles formed on the mould wall could be broken away and moved into the melt, promoting the nucleation of the carbide. The forced convection also helped in faster cooling of the melt, allowing the smaller nuclei to be stable and not re-melted. In addition, The Joule heat and Peltier effect caused by ECP influenced the carbide refining efficiency. Such heat played very minor role at high cooling rate but a major role in low cooling rates. Due to the heat effects, the fluctuations at the solid–liquid interface melted away, making it smooth and globular [46]. Zhou et al. [50] also reported that ECP treatment reduced the size of primary carbides to ~ 20 μm when applied near liquidus for long processing time. However, carbides will coarsen if the processing time was too long.

Geng et al. [47] applied an ECP of 500 Amperes to an HCCI melt between 1355 °C and 1337 °C, before solidification began in an alundum tube placed in muffle furnace. Noticeable reduction in the longitudinal size from 800 μm to 200 μm and the transverse size from about 200 μm to 100 μm were observed as shown in Fig. 5. Such refinement of the carbides led to a slight increase in microhardness [47].

To understand the mechanism by which the carbide was refined with ECP, Geng and coworkers [47] proposed two hypotheses. First, the application of ECP led to a distortion of the external electron layer of crystal due to as illustrated in Fig. 6. It was because of the difference in behaviour of ions. With the same ECP, different ions such as Fe and Cr with different specific charges gained different energies. Generally, Fe ions gained more energy than Cr ions and were easier to combine with crystal at the nucleation stage [47]. Initially, due to higher cohesive energy between Cr and C, the crystal embryo at the nucleation stage tends to combine with Cr available at the solid–liquid interface as shown in Fig. 6a However, after application of ECP, more high energy Fe ions were available to the crystal embryo than the Cr ions. This led

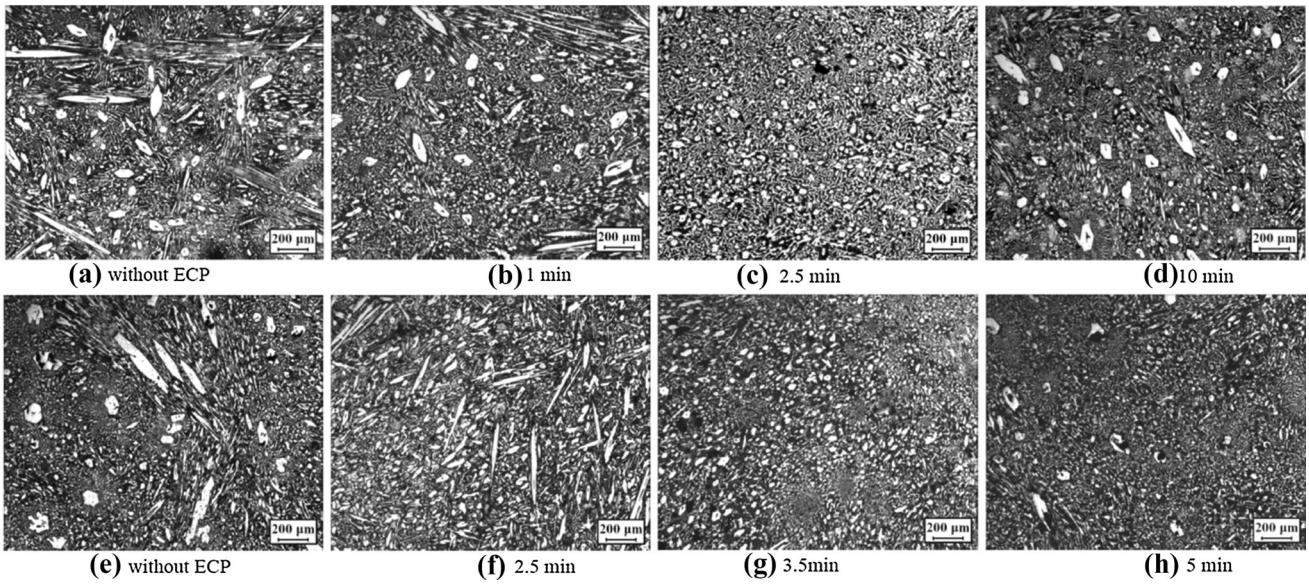

Figure 4 Solidification microstructures of the Fe-22.41Cr-4.2C HCCI with and without ECP treatment at different times with pouring temperature of 1350 °C (**a**, **b**, **c**, **d**) and 1360 °C (**e**, **f**, **g**, **h**). Adapted with permission from reference [46]. Copyright 2012, Trans Tech Publications.

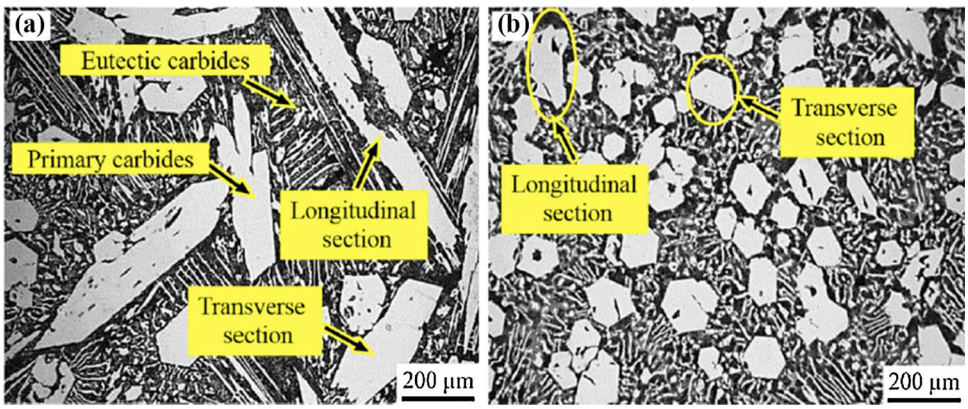

Figure 5 Morphology of Primary Carbides in Fe-19.4Cr-3.84C alloy with **a** Non ECP and **b** ECP. Adapted with permission from reference [47]. Copyright 2019, MDPI.

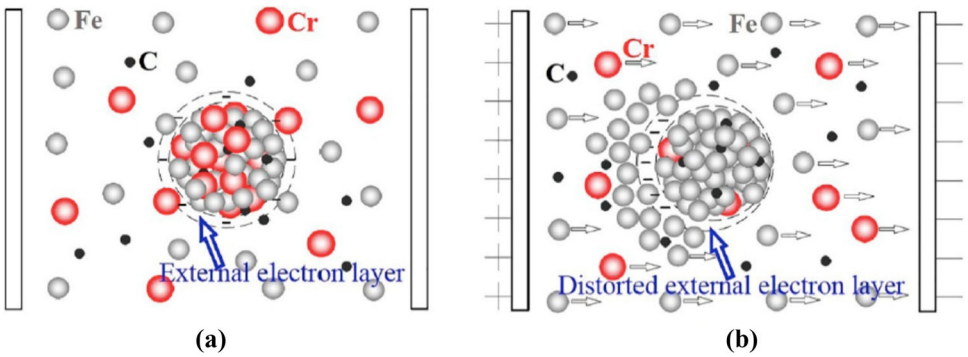

Figure 6 Schematic illustration of a carbide embryo growth during solidification of Fe-19.4Cr-3.84C HCCI **a** without ECP; **b** with ECP. Adapted with permission from reference [47]. Copyright 2019, MDPI.

to a decrease in Cr content in each crystal, which caused the distortion of the external electron layer as shown in Fig. 6b. Such distortion led to freeing up of atoms in the melt, which could combine to form new crystal embryos [47]. Second, as a consequence of the distortion of the electron layer, the content and distribution of chromium in the primary carbides were varied by the ECP as demonstrated in Fig. 7. At the

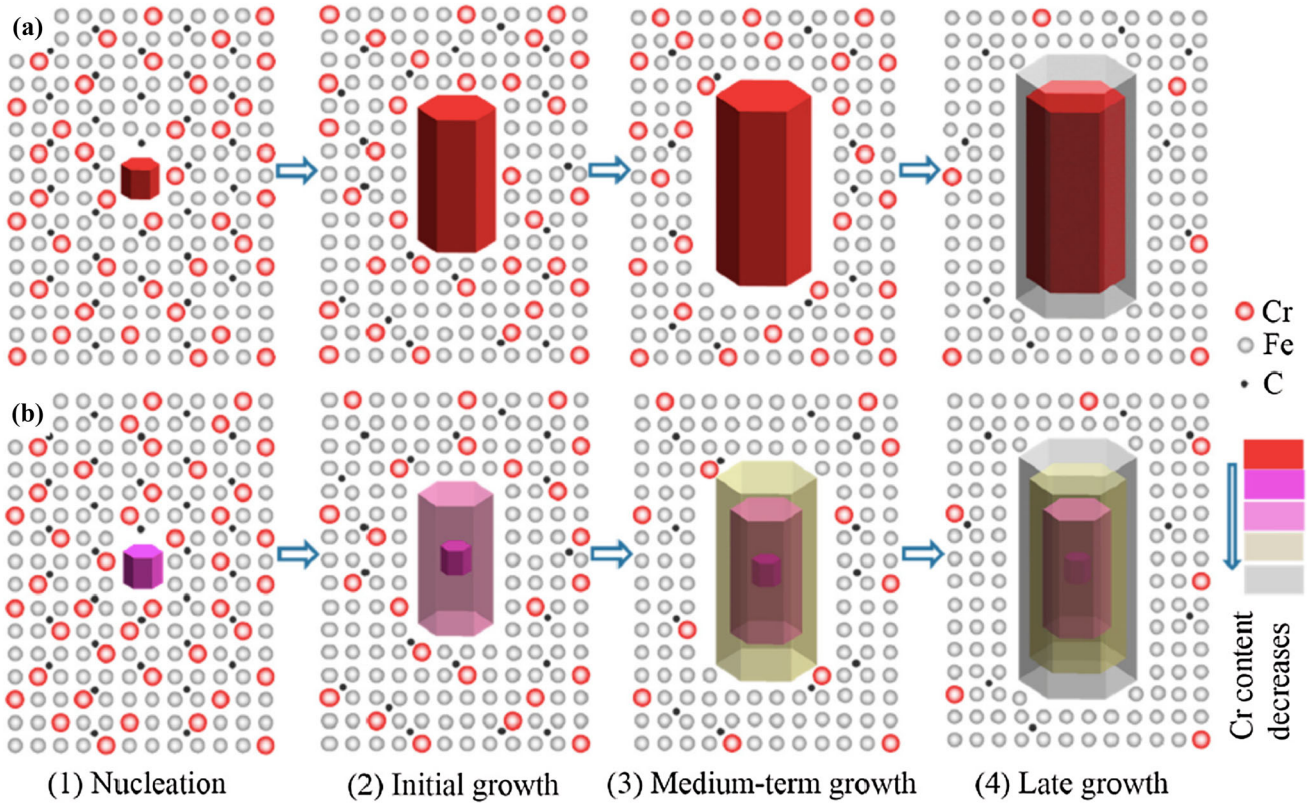

Figure 7 Schematic illustration of growth of primary carbides during solidification of Fe-19.4Cr-3.84C HCCI **a** without ECP; **b** with ECP. Adapted with permission from reference [47]. Copyright 2019, MDPI.

nucleation stage, samples with ECP had more carbide nuclei than in the non-ECP sample as ECP led to lower Cr content in the carbide nuclei. However, at the growth stage, in the samples without ECP, as the carbide contained higher Cr content than the nominal concentration of the alloy, which led to depletion of Cr at the solid–liquid interface as shown in Fig. 7a, while in the samples with ECP, there were Cr-rich carbide nuclei surrounded with high energy Fe ion readily available at the interface. Growth of the carbide resulted in Cr-enrichment at the core and depletion around the edge. This is because the higher energy of Fe ions increased the concentration of Fe at the solid–liquid interface. This caused the decrease in Cr content in the carbide as shown in Fig. 7b. In addition, this integration of Fe atoms in the primary carbides also decreased the lattice parameters of carbides due to the formation of $(Fe,Cr)_7C_3$ and led to decrease Cr content from centre to surface of the carbides [47].

Although ECP method is effective, the major limitation is how to scale up in industry. Generally, the HCCI parts are large up to a few metres in mining and mineral equipment and are made through sand casting. It is a great challenge to apply the ECP to such big castings.

Dynamic solidification process

Dynamic solidification is to elevate the casting into a dynamic state by either vibrating the casting or the mould during the initial stages of solidification. This causes turbulence in the melt, and its mechanical effect leads to the fragmentation of previously formed carbide that is loosely attached to the mould, acting as new nuclei. This leads to refinement in the casting [59]. It can be broadly classified into three categories in terms of the dynamic source used, namely ultrasonic, electro-magnetic and mechanical vibrations. The grain refinement process using dynamic solidification is well known and has been widely applied in light metal alloys [60–62]. The major advantages of introducing vibrations into the casting include increase in fluidity, refined microstructure, more homogeneity, improvement in mechanical properties, less porosity and cavities [62].

Many researchers have also tried to refine the carbide in high-chromium cast irons by introducing vibrations, leading to dynamic solidification of the melt [63–68]. Gittus [63] attributed the change in morphology of primary carbides caused by vibration to the replacement of primary carbides with primary graphite upon vibration, and also to the favourable growth of iron–graphite eutectic. The cause of these two effects was attributed to the increase in nucleation rate. However, this explanation not only lacked the evidence but also contradicted to the theory as the formation of primary carbides from the melt is governed by thermodynamics and mechanical vibrations cannot lead to phase change. Nofal et al. [64] poured the hypereutectic HCCI melt into two different moulds. One was static mould while the other mould was vibrated for 3 min from the start of the pouring using a mechanical vibrator with a frequency of 50 Hz and amplitude of 900 μm. Significant refinement in primary carbides was observed in the ingot cast with the application of mechanical vibrations as illustrated in Fig. 8. The size of the primary carbides decreased from 166 μm to 45 μm while the volume fraction increased from 48 to 52% [64, 65]. The carbide refinement mechanism of dynamic solidification process can be well understood in terms of the Chalmers Free Chill Crystal Theory (more details in "Chalmers free chill crystal theory" section). Additional nuclei could be introduced through two possible paths. First, when the mould is in dynamic state, the initially nucleated carbide crystals detach from the mould walls. They were then carried into the centre of the melt by convection in the liquid. They may act as nucleant for primary carbide. Second, the brittle carbide might break-away from the growing carbide crystal due to the impact caused by the dynamism in the liquid. The fragmented crystal, if stable enough, can either grow on its own or serve as a substrate for nucleation of primary carbides [60, 64]. Theoretically, the volume fraction of primary carbides in the casting is governed by thermodynamics and should remain unchanged in case of both static and dynamic solidification for a specific alloy. The increase in volume fraction was highly likely attributed to the inaccuracy to measure area fraction that was used to represent volume fraction because the experimental error of measurement could be higher when the carbide was refined. Huang, Z.F., et al. [68] reported that primary carbides were much finer when dynamic solidification was done under the pressure of 150 MPa, which led to the increase in toughness and wear resistance. The authors have neither quantified nor discussed the scale of refinement and effect of change in pressure. Moreover, the carbide refinement was attributed to the activation of BN coating, which is commonly used to coat the internal walls of mould. As BN coating has disassociating characteristics with respect to carbides, the detachment of carbide from mould walls during casting was facilitated, leading to the formation of more nuclei. Some researchers [44, 69] have experimented with slope cooling body method to refine the primary carbides. The mechanism involves a high-temperature melt flowing along a slope cooling body. In the process, a lot of crystalline carbides formed on the surface which are subsequently dissociated and swept with the melt in to the sand mould to inoculate the nucleation of carbide, and therefore fine structure was obtained after solidification. However, at high pouring temperature, the primary carbides were coarsened, while at low pouring temperature, the alloy had a lot of shrinkage porosities due to poor compensation ability of the melt [44]. Hence, the method does not produce any significant improvement in the toughness of the alloy.

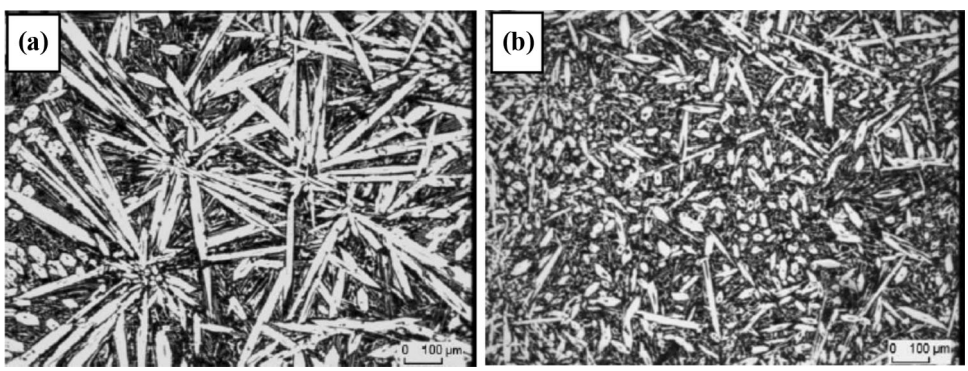

Figure 8 Optical Microstructures of the Fe-15Cr-4.3C HCCI obtained from **a** static solidification and **b** dynamic solidification. Adapted with permission from reference [64]. Copyright 2010, Trans Tech Publications.

Heat treatment process control

Like all other metallic materials, the properties of HCCIs are governed by their microstructure. In the presence of severe and repetitive-impact environments, HCCIs with austenite matrix can either undergo localized premature failure or failure of the whole casting [38]. The size, shape and distribution of primary carbides do not undergo significant change during heat treatment [70], because primary carbide forms directly from liquid, but heat treatment is most commonly done at solid. In addition to the primary carbide that is generally not changed during the subsequent heat treatment process, microstructure control of the matrix is also crucial to achieve optimal performance. For most HCCIs, the matrix in as-cast condition is stable austenite. Hence, a destabilization heat treatment is normally applied to the castings to reduce the alloy content of the austenite, resulting in precipitation of secondary carbides within the matrix. The carbides formed could be M_3C, M_7C_3, $M_{23}C_6$, which causes the depletion of alloying elements so that on cooling the austenite matrix can fully or partially transform to martensite [6]. The precipitated secondary carbide improves the strength of the austenite matrix and provides better support to the eutectic carbides [72]. Usually, destabilization treatment of HCCIs is done at temperatures above 1100 °C for 1–4 h followed by tempering [73]. The resultant microstructure is composed of eutectic and secondary carbides in a matrix of martensite [74].

Considerable studies have been done to investigate the effect of heat treatment on properties of HCCIs [70, 71, 75–81]. Pierce [74] found that destabilization at high temperatures up to 1025 °C had no effect on the morphology of the M_7C_3 carbides. It was observed that heat treatment can only slightly change the size but not the shape of the primary carbides. Hinckley et al. [71] heat-treated Fe-24.9Cr-5.18C HCCI at an elevated temperature of 1200 °C for one hour followed by water quenching. They observed slightly rounded off the carbide. It is because the destabilization treatment is usually done below the solidus temperature [71, 82, 83]. The improvement in properties resulted from heat treatment was mostly due to the changes in the carbide type and volume fraction of the precipitated phases in the matrix [3, 6, 70, 73, 79, 82, 84–88]. Kim, Lee and Jung [70] did heat treatment on the Fe-31Cr-2.8C alloy by austenitizing it at 1050 °C. The samples were air-cooled and oil quenched, respectively. They reported an increase in wear resistance resulted from the decrease in hardness difference between the carbide and matrix as the latter transformed from austenite to martensite. However, fracture toughness decreased due to the formation of martensite as the crack initiated at carbides cannot be effectively prevented by the matrix. Liu et al. [78] examined a Ti-containing Fe-17.4Cr-4.01C HCCI by heat treating at 900 °C, 1000 °C and 1050 °C for 2 hr and 6 hr, respectively. They observed an increase in number of M_7C_3 carbides with size greater than 11.2 μm after high destabilization at higher temperature, and an increase in number of secondary carbides with size less than 1 μm if destabilized at lower temperature, as shown in Fig. 9. This is because when holding at higher temperature for longer period, coarsening of carbides i.e. primary, eutectic and secondary, occurred [78]. The martensite was also refined at low destabilization temperature as compared to other cases. In addition, they found that increasing holding time decreased hardness and increased wear resistance due to coarsening of M_7C_3 carbides and increase in the matrix toughness, respectively. However, both hardness and wear resistance increased with lower destabilization temperature due to dispersion of M_7C_3 carbides along with secondary carbides in the martensitic matrix.

Modification of primary carbides in high-chromium cast irons through addition of modifiers

In addition to process control, melt treatment is the most cost-effective and practical approach to modify the morphology of the primary carbide in HCCIs. In addition to degassing, deoxidization and alloying, melt treatment in a foundry also includes modification and inoculation treatment. It means adding modifying solutes to restrict the growth of the secondary phase, which can be carbide, boride, nitride and intermetallic compounds depending of the composition of alloys, and to add inoculants that promote the heterogeneous nucleation of the secondary phase. Laird's study [37] demonstrated that addition of modifiers significantly changed the morphology of primary/eutectic M_7C_3 carbides which grow very fast along the preferred growth axis during solidification in all HCCIs, including

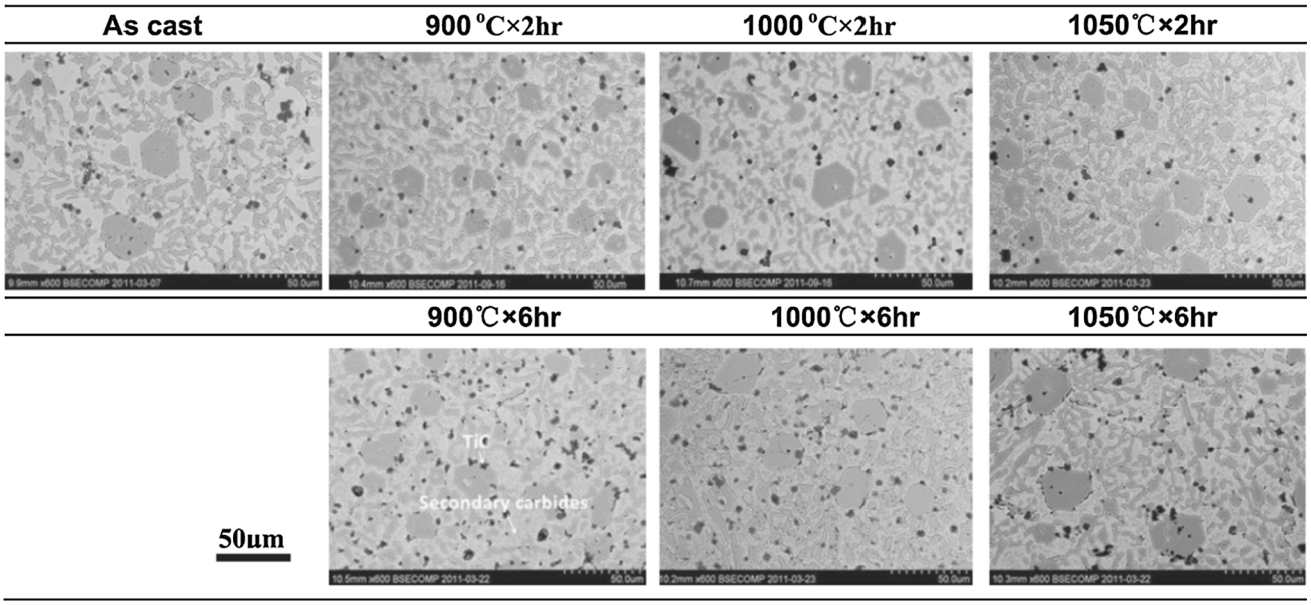

Figure 9 SEM Micrographs of the Ti containing Fe-17.4Cr-4.01C HCCI after destabilization heat treatments at various temperatures for different hours. Adapted with permission from reference [78]. Copyright 2012, The Iron and Steel Institute of Japan.

hypoeutectic (Fe-15.3Cr-3.1C) and hypereutectic (Fe-28.8Cr-3.2C).

Addition of solutes during modification/inoculation treatment differs from the alloying treatment. In HCCI, except for Cr, other common alloying elements are Ni, Al, V, Mo, W, etc. Their roles are to form carbides and/or intermetallic compounds and/or to increase the hardenability of the matrix. But, the common modifying solutes used in HCCIs include Mn, P, S, O, H, N, Ce, Mg, etc. [89]. When they are added, they can either act as solutes that affect the formation of constitutional undercooling zone in the front of the solid–liquid interface, altering the growth manner of the carbide, or react with atmosphere or other elements in the melt to form compounds, which can act as nucleants, promoting the nucleation of the primary carbides [90–92]. In addition, inoculants can also be externally added in the form of particles [41, 93].

Solute additions can be made using various methods, which may affect the homogeneity of the melt. Zhi et. al added the modifying agents by placing their powder in the bottom of the ladle before pouring the liquid metal in the sand mould [41]. However, such additions using powders are associated with a high possibility of uneven distribution or agglomeration of powder particles in the melt, resulting in high variability of pouring temperature, etc. [94]. This may lead to the inhomogeneity of the refinement and non-uniform microstructure. The most common method to add solutes is mechanically press the solutes into the melt using pure metal (rarely used) or a master alloy that is an Fe–M (where M = Mn, N, Ti, V, etc.) alloy [95–97]. This method ensures the homogeneity of the solutes dissolved in the melt. Another method is to place a layer of inoculant or particles to be added at the bottom of the ladle before transferring the melt into it [98]. This method cannot ensure fully and homogeneously mixing. Some particles need high temperature to dissolve in the melt, which maybe not be achievable in the ladle. Furthermore, the melt in ladle cannot be stirred to homogenize the melt. Several researchers have also introduced inoculants to the liquid HCCI in the powder form [99]. The major drawback of this method is the likelihood of segregation and agglomeration of the powder in the melt, limiting dissolving of the powder when the inoculant is added.

Although considerable studies have been conducted on the role of inoculants in grain refinement of cast light alloys [100–104], and a number of theories/models have been developed to understand the mechanism, the work on primary carbide of HCCIs is relatively limited. There is still no inoculant available for commercial use. In this section, some of the reported inoculants and solutes are reviewed and discussed.

Effect of adding nucleants on primary carbides in high-chromium cast irons

Influence of addition of TiC and TiBAl

In order to refine the coarse primary M_7C_3 carbides in HCCIs, other carbides have been considered as possible inoculants. Fu et al. [93] did not specify the basis but added TiC particles to a Fe-19.99Cr-4.03C hypereutectic HCCI. As shown in Fig. 10, 1.0 wt.% TiC particles addition led to the decrease in size of primary M_7C_3 carbides by 60%. Addition of over 1.0 wt.% did not lead to further refinement. Although the carbide refinement efficiency is high, in this work, addition of TiC was conducted through deposition of a TiC layer at the bottom of the ladle, followed by and stirring the melt with a steel bar. Dissolving the TiC particles homogenously in the melt is questionable.

Yilmaz and Teker [77] tried TiBAl as a carbide modifier of the Fe-17.2Cr-4.21C HCCI. Although microstructure showing the carbide modification was not reported, inoculation treatment with TiBAl up to 1 wt.% led to increase in impact toughness with no significant change in hardness. Further investigation may be needed to expose the potency of this carbide modifier.

TiC, with a melting point of 3160 °C, is very stable in liquid HCCI. Therefore, it can possibly act as a substrate for heterogeneous nucleation of primary carbides. Many studies have used two-dimensional lattice misfit model to calculate the lattice misfit between TiC and M_7C_3 carbides to understand the mechanism of carbide refinement by TiC particles. Wu et al. [105] and Huang et al. [106] reported a lattice misfit of being 1.32%, while the other studies

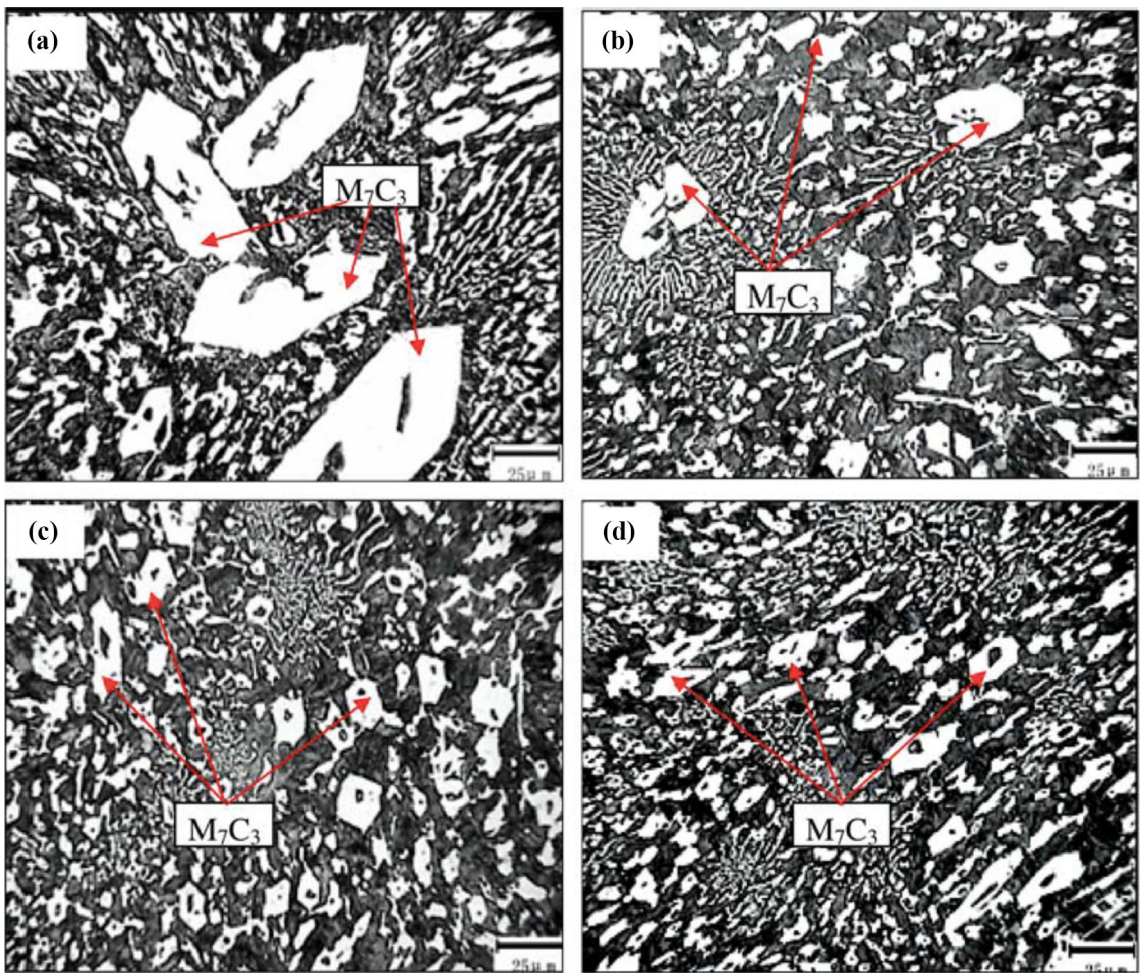

Figure 10 Microstructure of the Fe-19.99Cr-4.03C HCCI taken from 1 mm below the surface of ingots with various amount of TiC particle additions. **a** 0 wt.% TiC, **b** 0.5 wt.% TiC, **c** 1 wt.% TiC and **d** 1.5 wt.% TiC. Adapted with permission from reference [93]. Copyright 2009, Springer Nature.

[93, 107, 108] showed it was 8.4–8.6%. The difference in calculated lattice misfit was attributed to the different low index planes used in the calculation, which is detailed in "Two-dimensional lattice misfit model" section. But, although the resorted results indicated that TiC can refine primary M_7C_3 carbides, its refining efficiency is not high. This can be verified using the edge-to-edge matching model as detailed in "Edge to edge matching (E2EM) model: a successful case" section. Adding TiBAl alloy might enable the reaction of Ti with carbon or nitrogen in the HCCI melt to form TiC or TiN or Ti(C,N) [109], could act as heterogeneous nucleation substrate for primary carbides. Ding et al. [109] reported the lattice misfit between Ti(C,N) and M_7C_3 carbide being $8.46\% \sim 9.74\% < 12\%$; thus, Ti(C,N) can also potentially refine the primary carbides.

Effect of boron carbide

Borrowing the idea from light alloys, where TiB_2 is commonly used to refine the grains of cast aluminium alloys [110, 111], boron carbide was tested to promote the heterogeneous nucleation of primary M_7C_3 carbides and modify the carbides in HCCIs [98, 112, 113]. Kopyciński [98, 112] modified the Fe-24.5Cr-3.4C HCCI with boron carbide, crushed steel scrap and both of them. But, only the addition of boron carbide with steel scrap led to refinement of carbides and increased in hardness and wear resistance of the alloy, which was accompanied with reduction in strength. The alloy needed subsequent heat treatment to regain strength. The refinement of primary carbides occurred because unknown particles were introduced into the melt by the reaction between boron carbide and crushed steel scrap, which served as the heterogenous nucleation site for the carbides [112]. Studnicki and Jezierski [113] also experimented with boron carbide by inoculating it in a HCCI and compared its efficiency with niobium, vanadium, rare earth and nitrogen. Dissolution of boron carbide in the melt was observed, which led to negligible carbide modification as boron carbide itself does not act as a substrate for nucleation of primary carbides. It reacts with other reactive elements such as Nb, V to form various carbides, contributing to the refinement of primary carbides through promoting heterogeneous nucleation.

Role of rare earth (RE) oxides

Rare earth (RE) oxides have been considered as another effective carbide modifier in HCCIs, including hardfacing alloys [114–116]. A study by Yang et al. [116] on La_2O_3 showed that addition of La_2O_3 up to 0.78 wt.% led to the decrease in size of primary carbides from 13.43 μm to 11.37 μm and increase in fraction of eutectic carbide as shown in Fig. 11. As a result, the wear resistance was enhanced. Addition over 0.78 wt.% La_2O_3 led to coarsening of the primary carbides and deterioration of properties [116]. But, Zhou et al. [117] observed refined primary carbides even up to 6 wt.% La_2O_3 was added to a Fe-23Cr-4C HCCI. The refinement of primary carbides was attributed to heterogeneous nucleation of carbide on the La_2O_3 particles [115, 118]. It was found by Zhou et al. [117] that when La_2O_3 is introduced in the melt, it formed $LaAlO_3$ type inclusion, which was responsible for the refinement of primary carbides. They calculated the lattice misfit between $LaAlO_3$ and M_7C_3 being 8.37%. As this value is less than 12%, therefore, $LaAlO_3$ was considered as heterogenous nucleation site for primary carbides.

Hao et al. [114] added a mixture of RE oxides (oxides of Ce and La > 98%). which led to refinement and periodization of the primary carbides. 90% reduction in area fraction and 67% reduction in perimeter of primary carbides were observed with an addition of up to 4 wt.% RE oxides. The role of Ce_2O_2S in the nucleation and refinement of primary carbides was discussed based on calculating the lattice misfit between Ce_2O_2S and M_7C_3, which is 6.2%. As this value is less than 12%, Ce_2O_2S is moderately effective and can serve as the heterogenous substrate for primary carbides. But, the effects of La as solute seem not significant.

Effect of solute additions on the modification of primary carbides in high-chromium cast irons

Titanium additions

Early work by Wu et al. [105] and Zhi et al. [119] has shown that 1.5 wt.% Ti addition led to refinement of the primary M_7C_3 carbide from more than 10 μm to less than 4 μm different HCCIs. Chung et al. [99] added various levels of Ti ranging from 0 wt.% to 6 wt.% into an Fe-25Cr-4C alloy and noticed the

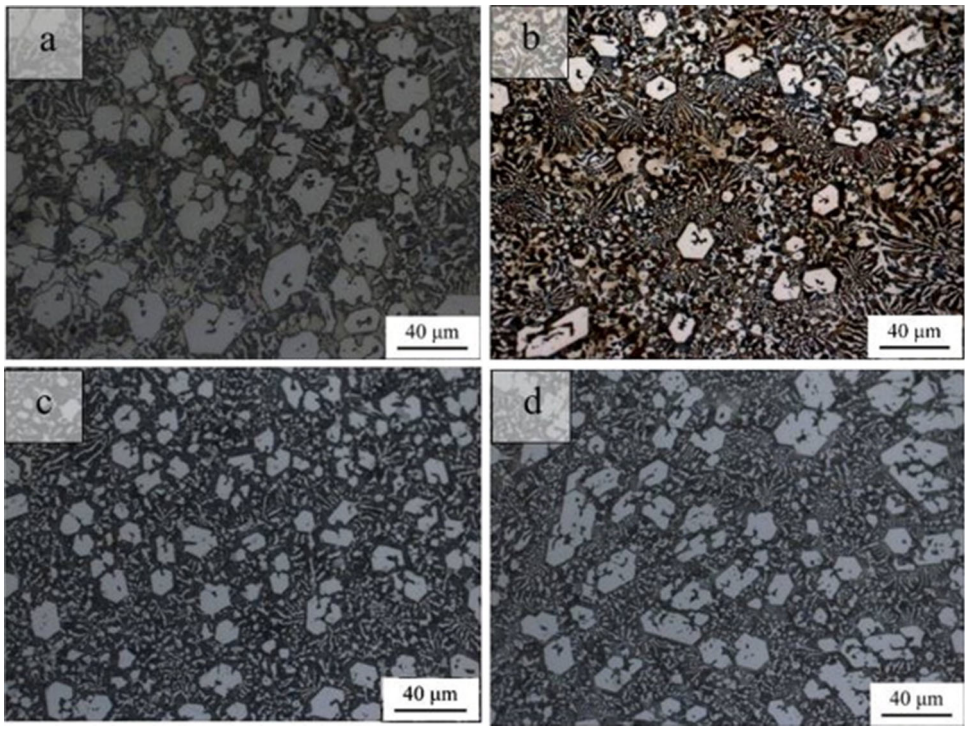

Figure 11 Microstructure of the Fe-11Cr-4.88C HCCI with various La_2O_3 additions. **a** 0 wt.% La_2O_3, **b** 0.39 wt.% La_2O_3, **c** 0.78 wt.% La_2O_3 and **d** 1.17 wt.% La_2O_3. Adapted with permission from reference [116]. Copyright 2014, Elsevier.

transition of the alloy from hypereutectic to hypoeutectic the addition level was over 2 wt.%. Liu et al. [42] added 1.5 wt.% Ti to an Fe-17Cr-3.79C HCCI and reported a decrease in the size of the primary carbides, from 151.9 μm to 53.9 μm (64% reduction) as shown in Fig. 12. All these authors observed the formation of TiC prior to the M_7C_3 primary carbide in HCCI melt, which not only refined the primary carbide, but also consumed the carbon in the HCCI, because Ti is a strong carbide forming element. Thus, Chung el at [99]. questioned the use of Ti as solute because upon addition of Ti over 2 wt.%, Ti consumes carbon from the alloy melt to form TiC. This moved the composition of the alloy from hypereutectic to hypoeutectic, leading to considerable reduction in the volume fraction of primary carbides. Ding et al. [109] added 0.4 ~ 0.5 wt.% titanium together with various concentrations (0.4, 0.54 and 0.2 wt.%) of nitrogen to an Fe-24.67Cr-2.3C HCCI. They observed more uniform primary M_7C_3 carbide formed owing to the Ti(C,N) particles that promoted the formation of the M_7C_3. Although TiN should thermodynamically have preference to form, the difference in concentration of added Ti and N enabled the formation of TiC through reaction of carbon with excess Ti. By increasing the

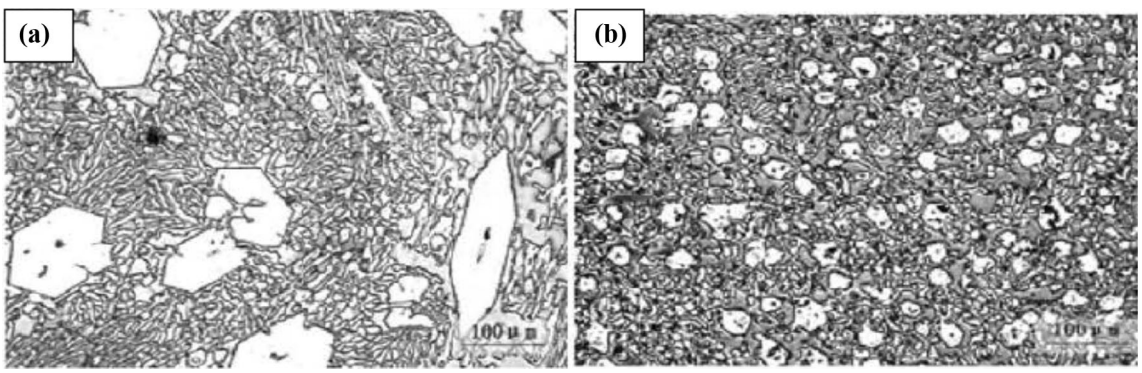

Figure 12 Micrographs of Fe-17Cr-3.79C after addition of **a** 0%, **b** 1.5 wt.% Ti. Adapted with permission from reference [42]. Copyright 2012, The Iron and Steel Institute of Japan.

concentration of nitrogen to 0.2 wt.%, refinement of primary M_7C_3 carbide by 60% was observed, which confirmed the role of TiN as the carbide modifier. Huang et al. [106] even reported a 75% reduction in size of primary carbides with 0.95 wt.% Ti addition and no further changes when the addition was above it.

As a strong carbide and nitride forming alloying element, Ti has been considered as a potential solute to refine the primary carbide in HCCIs. The refinement of primary carbides was attributed to the formation of TiC through chemical reaction of Ti and carbon, which provided inoculants in the melt for heterogenous nucleation of the M_7C_3 type of carbide. The ability of TiC to act as a substrate has been already discussed in "Influence of addition of TiC and TiBAl" section. Too much Ti addition could reduce the total volume fraction of the primary carbide as Ti consumed carbon in the alloys [42, 76, 97, 105, 107, 109, 119–123]. Wang et al.'s [124] work indicated that too many additions of carbide forming elements could even totally lead to suppression of formation of primary M_7C_3 carbides. As a result, the wear resistance of the alloys could be reduced. Hence, based on previous work, Ti addition to HCCIs should be optimized for different alloys to maximize its effect on property improvement.

Niobium additions

Niobium is another strong carbide forming element. Addition of Nb leads to the formation of NbC which further acts as inoculant to refine the primary and eutectic carbides. Like Ti, addition of excess amount of Nb consumes carbon in the melt, leading to reduction in volume fraction of primary carbides or change of microstructure of the alloy from hypereutectic to eutectic or hypoeutectic [64, 123, 125–130]. Chen et al. [128] observed a 60% reduction in the volume fraction of primary carbide when 1.4 wt.% Nb was added to the Fe-3.92Cr-3.92C HCCI. They also reported a refinement of the primary carbides from 50 μm to 20 μm, together with the shifting of the eutectic point towards higher carbon content, which led to further decrease in precipitation of primary carbides. Nb combines with the carbon in the alloy melt to form block-hook shaped NbC which can firmly hold the carbides in the matrix. Zhi et al. [125] obtained an average reduction of 44% in the average diameter of the primary carbides when the Nb content was increased from 0% to 1.5 wt.% in the Fe-20Cr-4C HCCI. As shown in Fig. 13, along with refining the size, the shape of primary carbides also became equiaxed. They attributed the refinement to the formation of NbC which reduces the carbon in the melt and decreased the volume fraction and size of the primary carbides. It was also noticed the presence of niobium on the boundaries of carbides, which was responsible for impeding the growth of primary carbides along preferential growth direction, leading to refined primary carbides. Nofal et al. [64] observed the formation of NbC, which consumed most of the carbon in the melt leading to decrease in precipitation of primary M_7C_3 carbides. The size of the primary carbides decreased from 166 μm to 35 μm when the Nb additions were increased to 2 wt.% in the Fe-15Cr-4.3C HCCI. The NbC particle also acted as a hindrance in the growth of primary carbides resulting in their refinement. Liu et al. [127] reported a 60–67% reduction in the diameter of the primary carbides from 30–50 μm to 10–20 μm when Nb additions were increased from 0 to 1.2 wt.% in Fe-26.3Cr-3.69C HCCI. By using thermocalc software, they noticed that upon addition of Nb, it reacted with carbon to form NbC, which formed prior to the primary carbide. They did calculations based on the first principles to determine interfacial energy and adhesion energy between $(0001)M_7C_3$ plane and $(111)_{NbC}$ and verified that NbC could act as a substrate, thus promoting the heterogenous nucleation of primary carbides [127]. Zhang et. al [108]. reported the carbide size reduction of 47% from 76 μm to 40 μm by adding 1.54 wt.% Nb into the Fe-24.63Cr-3.6C HCCI. In the same work, they also simultaneously added 1.19 wt.% Nb and 0.31 wt.% Ti which reduced the size of primary carbide from 76 μm to 22 μm in the same HCCI. They observed the formation of core–shell carbide formed by adding 0.29 wt.% Ti first and then 1.22 wt.% Nb. This core shell was smaller in structure and was found more dispersed than the (Nb, Ti)C. It was attributed to decrease in size of primary carbides to 11 μm. Based on these outcomes, Nb has strong potential as a better modifier for primary carbide in HCCIs. However, like Ti, it consumes carbon from the melt; therefore, optimal amount of Nb content should be determined and added to maintain the required properties.

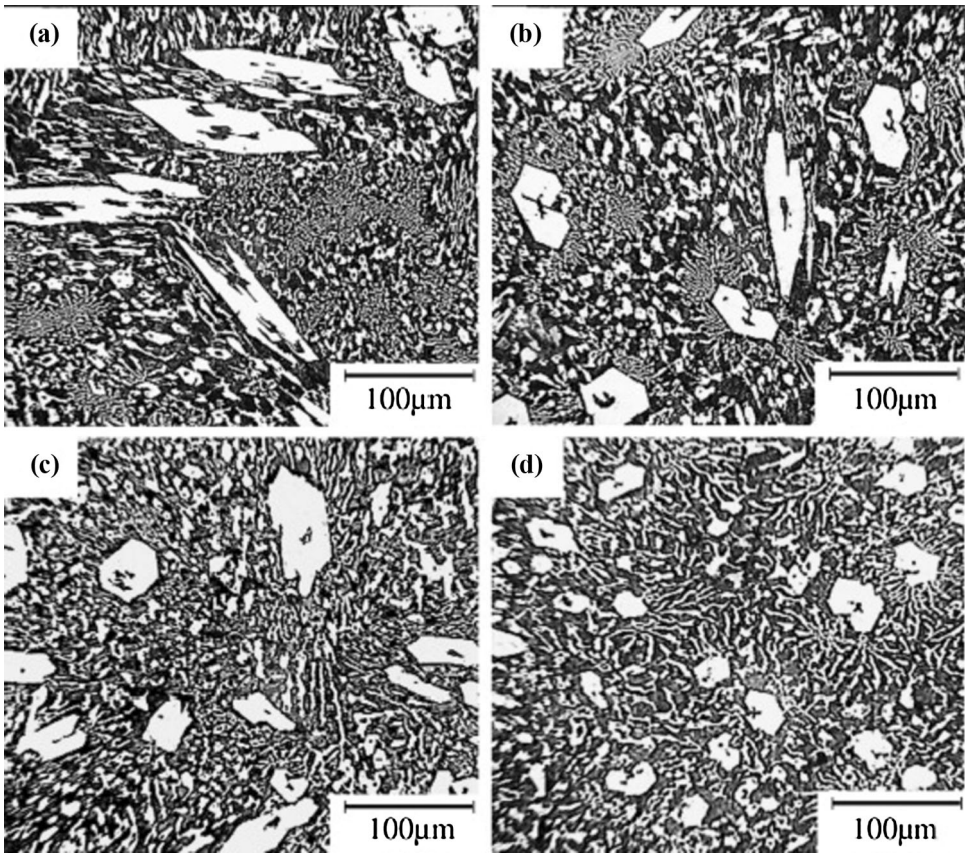

Figure 13 Microstructure of the Fe-20Cr-4C HCCI taken from 1 mm below the surface of the ingots with various Nb additions. **a** 0 wt.% Nb, **b** 0.5 wt.% Nb, **c** 1 wt.% Nb and **d** 1.5 wt.% Nb. Adapted with permission from reference [125]. Copyright 2008, Elsevier.

Vanadium additions

Addition of vanadium to Fe–Cr–C-based HCCIs leads to the formation of vanadium enriched M_6C_5 carbide before the primary M_7C_3 carbide [131]. As another strong carbide forming element, vanadium also consumes carbon in the HCCI melt. This leads a decrease in the carbon available for the solidification of primary carbide, which causes change in the volume fraction and "refinement" of primary M_7C_3 carbides in HCCIs [124, 129, 131–135]. Zhao et al. [136] added a combination of vanadium (0–0.3 wt.%) and rare earth (0–0.5 wt.%) in the Fe-26.2Cr-2.74C HCCI, and slight refinement of primary carbides was observed due to the formation of VC that acted as an inoculant, even though the authors did not quantify the size of primary carbides. To determine the effectiveness of VC for the heterogenous nucleation and ultimately, refinement of primary carbides, lattice disregistry between VC and primary M_7C_3 carbides was calculated to be 1.32% [136]. Work by Ma et al. [130] even did not identify any change in the morphology of primary carbide in the tested HCCI with composition of Fe-24.87Cr-3.21C. They added V along with other strong carbide formers such as Ti, Nb and Cr. V was primarily found to increase the hardness of the M_7C_3 carbides [130]. The addition of V along with other MC type carbide forming elements led to decrease and increase in liquidus and eutectic temperature, respectively [131]. Hence, it can be considered that vanadium has a relatively minor effect on the solidification of HCCI. However, excess addition of vanadium can suppress the formation of primary carbides as a result of formation of VC [124, 129]. Chung et al. [129] observed a relatively low variation on the solidification path of the alloy. The microstructure did vary, from hypereutectic to hypoeutectic with increase in addition of vanadium due to the formation of fine particles of VC. The decrease in carbon content resulted in low volume fraction of primary carbides while fine, in situ formed VC particles impeded the growth of carbides. The authors also reported the dissolution of V in the M_7C_3 carbide and solid-solution strengthening of austenite matrix, leading to increase in hardness.

Vanadium has also been commonly used to modify the morphology of eutectic carbide in hypoeutectic and eutectic HCCIs [14, 131, 134, 137, 138], even

though its effect on primary carbides in hypereutectic HCCIs is weak. Hence, it is considered that V is more suitable for hypoeutectic and eutectic HCCIs than for hypereutectic HCCIs.

Silicon additions

When silicon is introduced into Fe–Cr–C system, it does not form any carbides itself. But, it influences the volume fraction of the phases. Atamert and Bhadeshia [33] observed the presence of ferritic matrix and no austenite when 2 wt.% or more silicon was added to the Fe-34Cr-4.5C HCCI. Silicon was readily rejected from the carbide into the ferritic matrix during solidification of the primary phase. As a result, constitutional supercooling formed at the front of the growing primary carbide, which could lead to refinement of the carbides as described by the Winegard and Chalmers Theory and the Interdependency Theory as detailed in "Winegard and Chalmers Theory" and "The Interdependence Theory" Sections, respectively. It has been reported that addition of 8 wt.% Si modified the morphology of M_7C_3 carbide from needle like to equiaxed and promoted the formation of Cr_6C_4 during cooling via solid-state transformation. Zhi et al. [139] agreed that silicon plays a role in changing the morphology and refinement of primary carbides by either promoting its preferential growth or hindering its directional growth. However, the effect of silicon on the nucleation of M_7C_3 carbides is contradictory in the literature. Laird and Powell [88] reported, via image analysis, that addition of silicon up to 2.2 wt.% in Fe-17.8Cr-3C HCCI had no effect on the shape, volume fraction and morphology of the primary and eutectic carbides. It inhibited the nucleation but did not affect the subsequent growth of the eutectic carbides due to lower carbon content with increasing addition of silicon. While Shen and Zhou [140] observed an increase in carbide nuclei with increase in content of silicon to more than 2 wt.%. The mechanism was based on the higher binding energy of Fe to Si than that of Fe to C. This led to rejection of carbon into the melt for solidification of more carbide nuclei. Excess silicon additions decreased the eutectic temperature which increased the undercooling required for solidification of nuclei to refine primary carbides. Bedolla-Jacuinde and Rainforth [141] noticed the change in composition of alloy, from hypoeutectic to hypereutectic on addition of more than 4 wt.% silicon to Fe-16.8Cr-2.56C HCCI [142]. This was due to the increase in carbon equivalent of the alloy when excess silicon is added. As a result, the composition range of the alloy was shifted from hypoeutectic to eutectic and then finally, to hypereutectic, where M_7C_3 carbides are the first phase to solidify. This shift leads to substantial increase in the hardness of the alloy. In addition, it was also reported that addition of over 2 wt% silicon changed the matrix from austenite to ferrite in HCCIs, leading to decrease in wear resistance [33, 141]. Bedolla-Jacuinde, Rainforth and Mejía [142] studied the Si effect in more details and found that silicon promoted the transformation of austenite to martensite when Si addition was below 4 wt.% in Fe-16.8Cr-2.56C HCCI. However, addition more than 4 wt.% Si led to of the formation of ferrite and pearlite matrix directly in the as-cast HCCIs because Si is a typical ferrite-forming element in ferrous alloys. Powell and Randle [143] could not even specify the role of silicon, but postulated that it might affect the growth of carbides as they observed disconnected eutectic M_7C_3 carbides when 1.3 wt.% Si was added to Fe-18Cr-2.8C HCCI, which led to improvement in fracture toughness. This disconnection was attributed to the less strain induced between M_7C_3 carbides and the austenite matrix during the solidification of the alloy. Many studies agree to the solid solution effect of silicon, leading to increase in number and refinement of eutectic carbides and improvement in hardness and wear resistance of the alloys [141, 143–145] when proper amount of Si was added. Based on previous results, it is suggested by the current authors that Si addition should not excess 4 wt%.

Molybdenum additions

Unlike other carbide forming elements, such as Ti, V, Nb, W, molybdenum tends to form eutectic M_2C, M_6C and MC carbides [124, 129, 146–148], which consumes carbon in the melt. This carbon consumption shifts the carbon equivalent to eutectic or hypoeutectic range [124, 130]. As this type of carbides is very hard, it not only refines the primary M_7C_3 carbides, but also improves the hardness and wear resistance of the material [124, 129, 147]. Molybdenum, even with small quantities, can suppress the formation of pearlite [149]. Scandian et al. [147] reported that addition of over 3 wt.% Mo to a 32 wt.% Cr containing HCCI facilitated the precipitation of

eutectic M_6C carbide in ferritic matrix, which enhanced the hardness and wear resistance. The loss of volume during wear was mainly due to ferritic matrix. With the help of image analysis, it was confirmed that increase in Cr and Mo additions decreased the volume fraction of the matrix as a result of the formation of more carbides, such as primary and eutectic M_6C. However, Chung et al. [129] reported a different result. They found that 13 wt.% addition of Mo refined the primary carbides and produced a near-eutectic microstructure consisting of refined M_7C_3, MC and M_2C in the austenite matrix. This refinement was attributed to the consumption of carbon by Mo, which reduced the total volume fraction of primary carbides as compared to base alloy. They found that although Mo addition increased hardness of the matrix of the Fe-24.8Cr-3.72C HCCI, it was also associated with large volume loss during wear as compared to the alloys containing other carbide forming elements, such as Nb and V. This was attributed to the formation of brittle and interconnected Mo_2C carbides when Mo addition was over 6 wt.%, to which facilitated the crack propagation and lowered the wear resistance. However, opposite results were reported by Yamamoto et al. [150] that Mo addition did not modify the morphology of primary carbide in a Fe-25Cr-4.5C HCCI. As shown in Fig. 14, addition of various amount of Mo ranging from 0 to 15 wt.% into the HCCI showed no effect on the morphology of the primary carbides. With increase in the addition level, Mo either dissolves in M_7C_3 carbides, leading to lattice distortion or precipitated as Mo_2C carbides near the eutectic point in the final stages of solidification. Many other studies also verified that Mo addition did not improve the fracture toughness and/or wear resistance of the alloys [150, 151]. Hence, Mo seems not a suitable modifier to modify the morphology of primary carbide in HCCIs.

Tungsten additions

Like Mo, W, when added to HCCI, forms various tungsten carbides, including WC, W_6C, W_3C, which were found in the matrix and considerably increased the hardness and wear resistance of the alloys [122, 124, 152–154]. The more the tungsten added, the higher is the hardness and wear resistance [122, 152, 154]. Accordingly, additions of tungsten over 1.0 wt% lowered the toughness of the alloys. As a strong carbide forming element, tungsten consumes carbon and "refines" the primary carbides by decreasing its volume fraction. Over additions can lead to compositional shift to eutectic or hypoeutectic range [124]. Anijdan et al. [152] attributed better mechanical properties of a W-containing Fe-28.84Cr-3.03C HCCI to the presence of tungsten carbide in the matrix with increase in tungsten from 0% to 2.5 wt.%. Although tungsten carbides were observed, mechanisms of refinement of primary carbides were not discussed. Lv et al. [154] reported the refinement of primary and eutectic carbides with irregular distribution of carbides in the matrix in the as-cast structure when up to 2.75 wt.% W was added into Fe-24.45Cr-3.08C HCCI. This was resulted from the formation of WC_{1-x}, $W_6C_{2.54}$ and CW_3 along with Mo present in the alloy, which consumed carbon from the melt, leading to decrease in volume fraction of primary carbides. Furthermore, carbide formation in the melt also locally consumed carbon, and increased the martensite start temperature, leading to transformation of austenite to martensite, However, Yamamoto et al. [150] reported different results. They found that addition of W, even up to 15 wt.%, into a

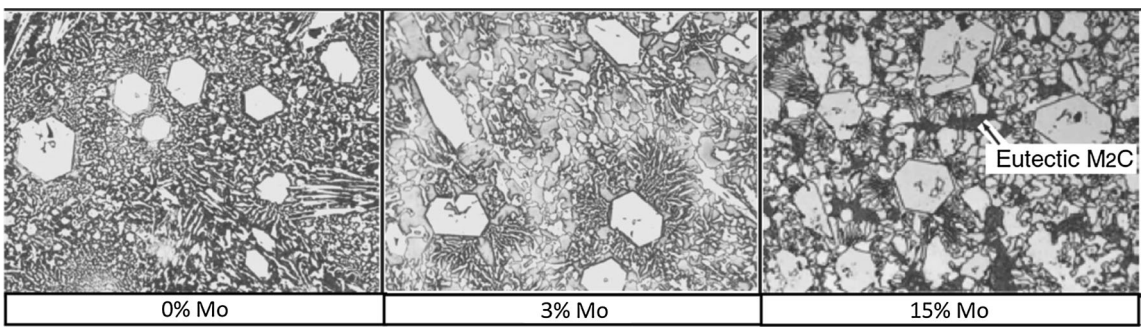

Figure 14 Effect of molybdenum addition on microstructure of the as-cast Fe-25Cr-4.5C HCCI. Adapted with permission from reference [150]. Copyright 2014, The Japan Institute of Metals and Materials.

Fe-25Cr-4.5C alloy, did not significantly verify the primary carbides as shown in Fig. 15. In addition, it was verified that just like Mo, W could also dissolve in M_7C_3 carbide by substituting the Fe and Cr atoms. This might cause lattice distortion of the M_7C_3 at high levels of W addition.

Role of rare earth (RE) elements as solutes in HCCIs

Rare earth elements are known to improve strength, ductility, fatigue strength and corrosion resistance in light alloys [155, 156]. In HCCIs, the optimal RE addition, including cerium, lanthanum and neodymium, was considered as 0.13–0.26 wt.%. RE elements generally have limited solubility in carbides and austenite; therefore they tend to form oxides and/or sulphides in meal melts as fine inclusions in solidified alloys [157]. However, due to the extreme difficulty to add REs into metal melts, the actual nominal addition is much higher than this amount. It is considered that inclusions formed through chemical reaction of RE elements with oxygen or sulphur in the melt can act as heterogeneous nucleation substrates for primary carbides [157, 158]. Depending on composition of the alloy, oxygen and sulphur in particular, either sulphides such as Ce_2S_3 or oxysulphides such as Ce_2O_2S, can form before solidification starts. Subsequently, they can facilitate the nucleation of primary M_7C_3 carbides, causing carbide refinement. Many studies have used two-dimensional lattice misfit model proposed by Bramfitt [159] to examine the suitability of Ce_2O_2S and Ce_2S_3 as heterogeneous nucleation substrates for the M_7C_3 carbides [95, 158, 160]. Qu et al. [158] added up to 1.5 wt.% Ce into a Fe-19.4Cr-4.17C HCCI and observed refined and spheroidized primary carbides. The refinement of primary carbides was attributed to the formation of Ce_2O_2S inclusions, which acted as heterogeneous nucleation substrates for the primary carbides. They reported the lattice misfit between Ce_2O_2S and M_7C_3 to be 0.69% and 1.6%. Zhou et al. [160] also observed a decrease in diameter of primary carbides, from 18 μm to 6.8 μm with addition of 2 wt.% ceria additive to a Fe-22-26Cr-4-4.2C HCCI. As inclusions of cerium have to be stable before the solidification of primary carbides, the authors evaluated all the possible oxides, sulphides and oxysulphides of cerium. On the basis of Gibbs free energy and XRD results, it was concluded that Ce_2O_2S inclusion is stable in the alloy melt before the solidification of primary carbides. The relatively low lattice misfit of 6.2–8.2% between Ce_2O_2S and M_7C_3 indicates the strong potential for the Ce_2O_2S particles to act as nucleant for the carbide. In addition, Zhi et al. [95] also observed the formation of Ce_2S_3, which acted as heterogeneous nucleation site for M_7C_3 in a Fe-19.4Cr-4.17C HCCI. They reported that the Ce_2S_3 inclusion is stable and has a lattice misfit of 4.5% with M_7C_3. The result showed that adding up to 1.5 wt.% Ce reduced the size of the primary carbide by 25% in the Fe-19.4Cr-4.17C HCCI as shown in Fig. 16. Additionally, due to low solubility of Ce in carbide and the matrix, the element segregates in front of the growing carbide at the solid–liquid interface. This leads to large constitutional supercooling, which might further facilitate in nucleation and refinement of primary carbides [95]. More details about this mechanism are discussed in "Winegard and Chalmers Theory" and "The Interdependence Theory" Sections.

It has been widely reported that RE addition enhanced the mechanical properties of HCCIs, such as wear resistance, hardness and impact toughness [95, 136, 160, 161]. But, Kawalec [95] reported that

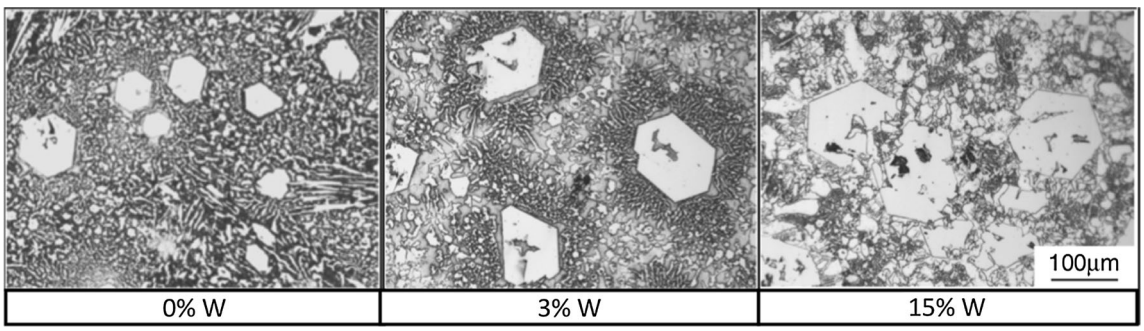

Figure 15 Effect of tungsten on the as-cast microstructure of the as-cast Fe-25Cr-4.5C HCCI. Adapted with permission from reference [150]. Copyright 2014, The Japan Institute of Metals and Materials.

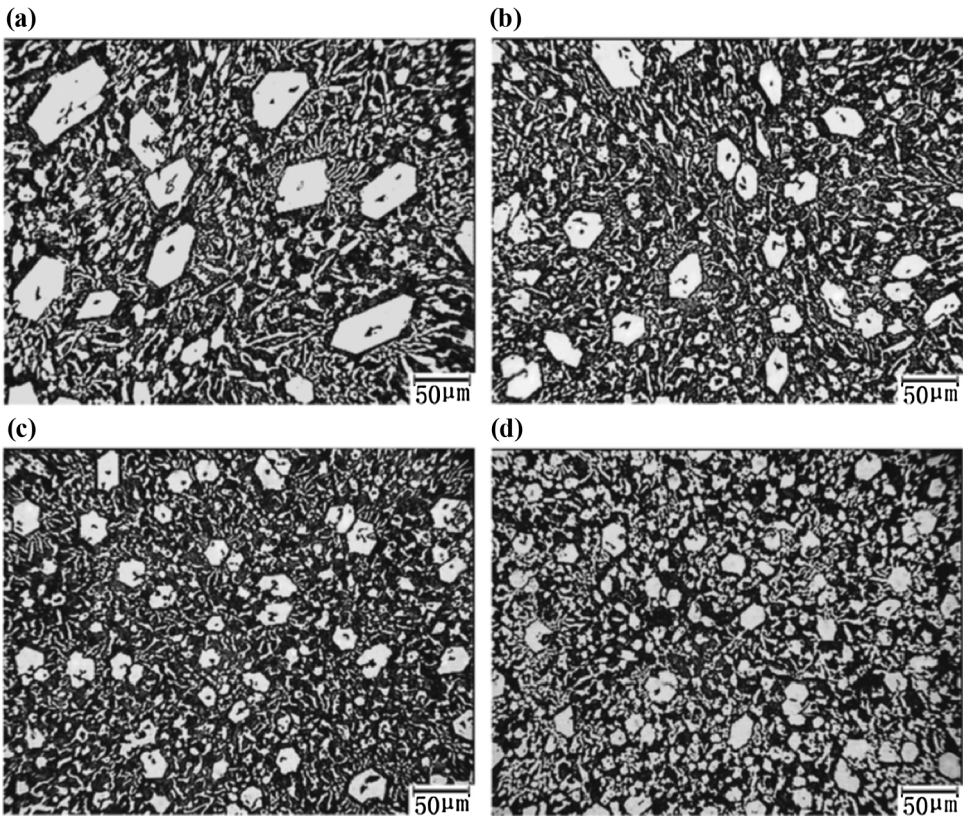

Figure 16 Micrographs of the Fe-19.4Cr-4.17C HCCI with various Ce additions. **a** 0 wt.% Ce, **b** 0.5 wt.% Ce, **c** 1 wt.% Ce and **d** 1.5 wt.% Ce. Adapted with permission from reference [95]. Copyright 2014, Elsevier.

addition of lanthanum in high alloyed HCCIs reduces tensile strength and slightly improves the ductility impact resistance of the alloys. Due to the lack of comprehensive studies of the roles of REs in different HCCIs, it is hard to draw any conclusions. But, the potency of REs in HCCIs is a research topic that is worth to work on.

Boron additions

In addition to the boron carbide (B_4C) discussed above, boron has also been added to HCCIs as solute since it is a common alloying element for ferrous alloys. Chung et al. [129] added various amount of boron ranging from 0 to 13 wt.% to a Fe-25Cr-4C HCCI. The modification of microstructure was different as compared to those with carbide forming elements, such as Ti, Nb. No significant impact on primary carbides was observed because of the high solid solubility of B in carbides. Boron readily dissolves in M_7C_3, $M_{23}C_6$ carbides by replacing the carbon atoms in the carbides and in austenite matrix, forming $M_7(C,B)_3$, $M_{23}(C,B)_6$ in addition to the formation of M_2B. As a result, the equivalent carbon content in the matrix was increased, which increased the volume fraction of primary carbide and more solidification of carbide nuclei. In addition, boron addition also leads to the transformation of austenite to bainite or martensite [129, 162]. This further led to the improvement in mechanical properties such as hardness of the alloy [144]. However, excess addition of boron enabled the formation of M_2B borides as shown in Fig. 17. Unfortunately, the actual roles of such boride are still unknown (Table 1).

Considerable work has been done to develop techniques to modify the morphology of primary carbide in HCCIs using the elements and compounds discussed above. But, only limited success was achieved. This is because high level of additions of the solutes could either lead to change in the composition of the alloy from hypereutectic to hypoeutectic or form brittle phases that lead to deterioration of mechanical properties. In addition, in the cases where the nucleants are not in situ forming, the external addition of inoculants is still a challenge. Furthermore, majority of the currently reported carbide modifiers are carbides that form through addition of strong carbide forming alloying elements except for a few oxides and nitride. In fact, these techniques have been widely used in austenitic grain

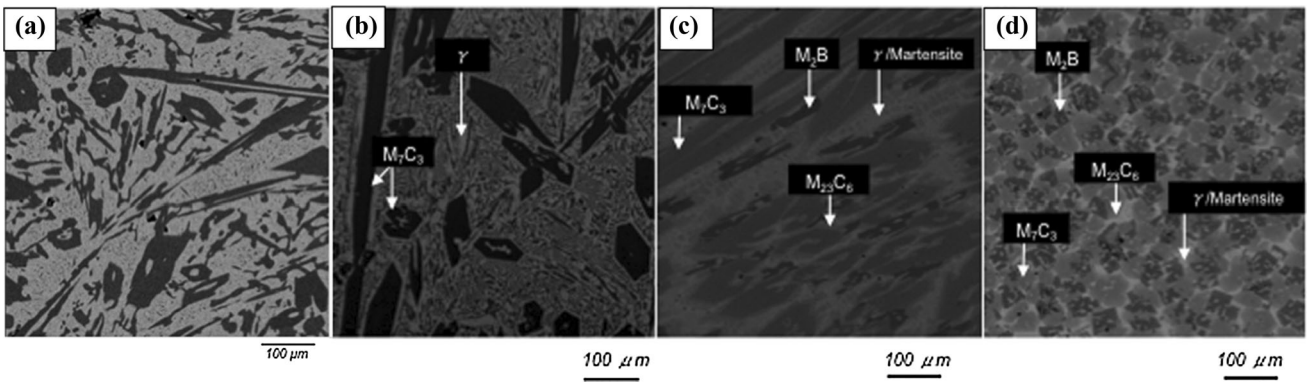

Figure 17 Micrographs of the Fe-25Cr-4C HCCI with various B additions. **a** 0 wt.% B, **b** 2 wt.% B, **c** 10 wt.% B and **d** 13 wt.% B. Adapted with permission from reference [129]. Copyright 2013, Elsevier.

refinement in steels. In addition, in light of the lack of comprehensive theories /models to understand the mechanisms of these available carbide modification techniques, almost all of them were developed through trial and error approach. Thus, the questions arisen are:

(1) Are the currently reported carbide modifiers optimal to modify the primary carbide in HCCIs?
(2) Are there more effective and lower cost modifiers that have not been discovered?
(3) How to identify and discover new and more effective modifiers?

To answer the third question, the present authors propose to apply the grain refinement theories/models well developed for cast metals in the recent years to identify new modifiers for the primary carbide in HCCIs followed by experimental validation. In order to reveal such a possibility, major grain refinement theories/models for cast metals are reviewed in the following section.

Theories/Models of grain refinement developed for cast metals and their application to high-chromium cast irons

Grain refinement not only can simultaneously improve the strength and ductility, but also can minimize the porosity and segregation of cast metals [62, 103, 163, 164]. Hence, it has been comprehensively studied and widely used in the foundry, light metals in particular. In the past decades, a number of theories/models have been developed to understand the mechanisms of grain refinement and to guide the discovery of new grain refiners. Majority of these theories/models were developed in cast aluminium alloys [90, 104, 165–168], and then were extended to cast magnesium alloy [61, 100, 101, 169–171], titanium alloys [172–175] and steels [163, 164, 176, 177]. Several review papers on grain refinement have been published in the past years. In this section, major grain refinement theories/models are briefed, followed by discussion on the possibility to extend these theories/models to HCCIs in order to understand the mechanism of primary carbide modifications and to discover new and more effective carbide modifiers.

Winegard and Chalmers Theory

In 1954, Winegard and Chalmers [178] proposed a theory based on constitutional undercooling resulted from the solutes that present ahead of the solid–liquid interface. When the solute, B, is rejected from the growing solid–liquid interface due to the different in solubility of the solute in the solid and liquid, variation of the solute concentration in the liquid as shown in Fig. 18a leads to change in liquidus temperature, T_0, of the melt adjacent to the interface as shown in Fig. 18b. The higher concentration of solute close to the interface lowers liquidus of the local melt compared with the regions far away from the interface. When the liquidus temperature gradient at the interface is larger than the real temperature gradient, constitutional undercooling occurs in the melt. Once the sum of the thermal undercooling and the constitutional undercooling in the melt excesses a critical undercooling, it paves the way for heterogenous nucleation on nucleants, which can be externally

Table 1 Summary of all the reported modifiers for the primary carbide in HCCIs

Function (Nucleant or Solute)	Element/ Alloy	Effect on refinement of primary carbides	Refining efficiency	References
Nucleant	TiC/TiBAl	Heterogeneous nucleation substrate for the M_7C_3 primary carbides	60%	[77, 93]
	Boron Carbide	Heterogeneous nucleation substrate for the M_7C_3 primary carbides.	–	[98, 112]
	La_2O_3	Heterogeneous nucleation substrate for the M_7C_3 primary carbides.	15–67%	[116]
Nucleant + Solute	Titanium (Ti)	Forms TiC which acts as nucleant for the primary M_7C_3 carbide	60–64%	[42, 97, 105, 119, 120]
	Niobium (Nb)	Form NbC which acts as nucleant for the primary M_7C_3 carbide Nb as a solute shifts the eutectic point to the right leading to decrease in precipitation of primary carbide	44–67%	[64, 123, 125, 126, 128]
	Vanadium (V)	Forms VC which acts as nucleant for the primary M_7C_3 carbide and V rich M_6C_5 carbide V as a solute decreases the solidification temperature leading to decrease in precipitation of the primary carbide	–	[124, 131–134]
	Tungsten (W)	Form MC, M_3C, M_6C during casting and M_2C in heat treatment Mostly found to strengthen matrix by refining the eutectic carbides Strengthening of the matrix as a solute. It dissolves in carbides leading to lattice distortion	–	[122, 152, 154]
	Rare Earth Elements (Ce, La)	Ce reacts with sulphur and oxygen in the melt to form Ce_2S_3 or Ce_2O_2S, which acts as a heterogeneous nucleation substrate for the M_7C_3 primary carbide La forms different types of inclusions in Fe–Cr–C alloys, which act as heterogeneous nucleation substrates for the M_7C_3 primary carbide	25–62%	[95, 157, 158, 160]
	Molybdenum (Mo)	Mo strengthens matrix by forming eutectic MC, M_6C and M_2C carbides, hinders growth of primary carbides by consuming carbon	–	[124, 129, 146–148]
Solute	Silicon (Si)	Si refines eutectic carbides and improves mechanical properties. Excess additions facilitates the formation of ferrite in the matrix, deteriorating wear resistance	–	[141–143]
	Boron	Dissolves in carbides and austenite to form $M_7(C,B)_3$, $M_{23}(C,B)_6$ and promote martensitic transformation	–	[129, 144, 162]

added or in situ formed. This "new" nucleation inhabits the growth of previously growing solid, leading to grain refinement [167, 178, 179].

This is the earliest and most popular theory developed to explain grain refinement in light metal alloys. According to the theory, the solidification starts on the walls of a mould, which is associated with a directional growth, resulting in columnar grains. Such growth leads to the formation of constitutional supercooling zone, in which "secondary" nucleation occurs on the nucleants within the constitutional undercooling zone. As a result, the directional growth is terminated and fine equiaxed grains form. In aluminium alloys, nucleation of α-Al commonly occurs on TiC, TiB_2, AlB_2 and (Al,Ti)B [90, 104]. In magnesium alloys, Mg nucleates on either Al_4C_3 or Al_2CO [180, 181].

This theory has been supported by a number of experimental observations for both aluminium and magnesium alloys [90, 182]. Some researchers

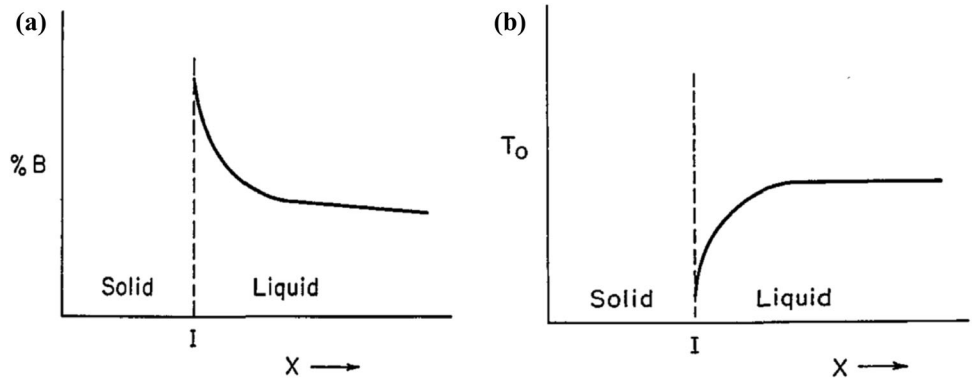

Figure 18 Schematic illustration of the formation of constitutional undercooling zone at the solid–liquid interface. **a** solute distribution and **b** liquidus temperature near the solid–liquid interface and constitutional undercooling zone. Adapted with permission from reference [178]. Copyright 1954, Metals Park, Ohio, American Society for Metals.

working with HCCI have also attributed that carbides, such as TiC, and nitrides, such as TiN, can act as nucleants for the primary M_7C_3 carbides [42, 76, 97, 105, 109, 119–121, 159]. However, this hypothesis has not been fully verified and commercialized carbide modifiers for HCCIs are still not available.

Chalmers free chill crystal theory

The Free Crystal theory was first proposed by Genders in 1926 and developed by Chalmers in 1963 [183, 184]. As per the theory, the "free" chill crystals nucleate on the mould wall when the melt is poured, and are subsequently swept into the melt. This leads to the formation of equiaxed crystals. Initially, the crystals nucleate on the mould wall and grow inwards the liquid accompanied with solute rejection to the front of liquid/solid interface when heat conduction occurs through the wall. Due to solute rejection, some of the crystals are detached from the mould wall or broken and become "free" crystals. Such free crystals, because of the solute gradient, have an interface temperature lower than the liquidus temperature of the rest of liquid, forming a constitutional undercooling layer surrounding individual crystals. Thus, they are protected from melting by the constitutional undercooling. The number of such protected crystals is higher for lower pouring temperatures and high solute content. These protected crystals are carried away from the mould wall by convection and turbulence, and continue to reject solute and grow in an equiaxed manner until impinged by each other. In the theory proposed by Chalmers, the convection in the melt plays a major role in the formation of equiaxed zone in the casting [179, 184].

Separation theory

In 1976, A. Ohno proposed the separation theory [185]. According to the theory, for pure metals, the crystals initially form and grow on the mould wall with the highest undercooling. They continue to grow until the adjacent crystals meet each other and form a shell on the mould wall as illustrated in Fig. 19a. The crystals do not separate from the mould wall after forming a consolidated shell on the wall. This is commonly called chill zone. Some crystal with preferred growth orientation that is normal to the mould wall will continue to directionally grow as the temperature lowers. As there are no barriers, such as the nucleation within the constitutional undercooling zone, the directional growth continues until they meet at the centre of the mould. Thus, the formation of equiaxed crystals is not observed in this case. For alloys, it is different. As Ohno stated [185] "equiaxed crystals in ingots are formed by the crystals that have nucleated on the mould wall having the growth of their roots restricted by segregation of the solute, and that they then separate in the stage prior to the formation of a stable solid shell". During solidification, the primary or the leading phase is the first to form on the mould wall as equiaxed crystals. The solute rejection surrounding each crystal suppresses the formation of the consolidated chill zone. They can then detach from the wall. This breakage from the mould wall might be due to vibrations or fluctuations

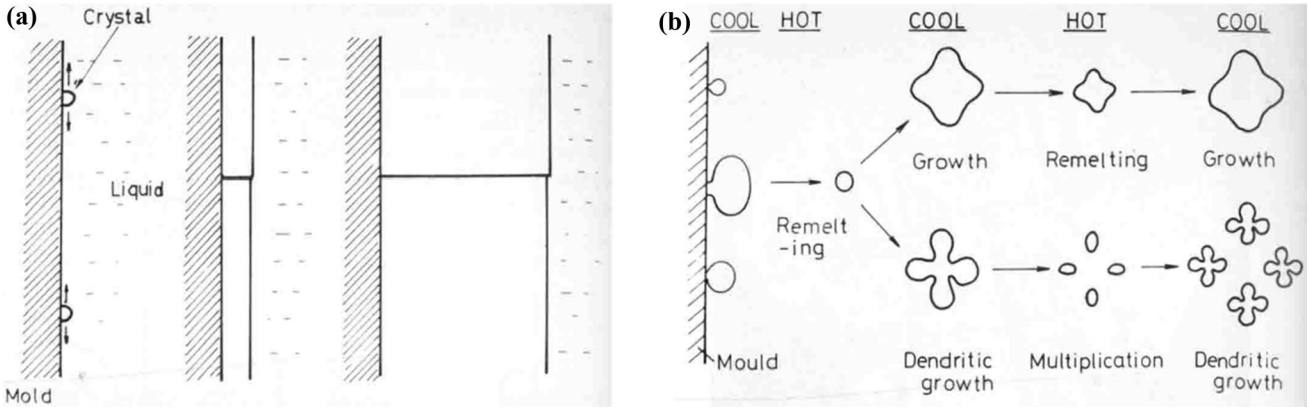

Figure 19 Ohno's graphical representation of growth of crystals **a** For pure metals, nucleation occurs on the mould wall, and then growth in meeting with adjacent crystals to form a shell on the wall; and **b** for alloys, crystals formed on the mould wall break away into the melt to grow as either necked-dendrite arms with fragmenting at high temperature to grow as independent crystals or separated crystals can partially re-melt at high temperature or grow at low temperature in alloys. Adapted with permission from reference [185]. Copyright 1977, American Foundrymen's Society.

in temperature, mechanical force caused by convection or thermal factors as illustrated in Fig. 19b. As the temperature of the melt decreases, the convection decreases, leading to the simultaneous formation of columnar zone along the mould wall and growth of either dendritic or equiaxed crystals near the centre. But, the growth of the columnar zone is stopped by the growing equiaxed crystals from the central region of the mould [179, 185]. This theory has been confirmed in various practical applications and in situ observations [179, 186–188].

For a hypereutectic alloy, as illustrated in Fig. 20, there can be different variations to the theory depending on the leading phase. In the initial stage, the primary phase and secondary phase will nucleate and grow in the melt and the mould wall, respectively, as in Fig. 20a1. The primary phase nucleates first after the melt is poured and then gets detached from the mould wall. If the primary phase is not the leading phase, then the columnar grains are preferred as in Fig. 20a2. If the leading phase is the primary phase or there are any pre-existing particles like detached primary crystals, grain refiners, in situ formation of primary particles for instance, the growth revolves around them, leading to the formation of equiaxed grains as in Fig. 20a3 [43].

Typical application of this theory was proposed by Laird and Dogan [43] who observed that the casting mainly comprised of columnar structure at high pouring temperatures. It is because of the fact that high pouring temperature is associated with large thermal gradient that promotes the growth of

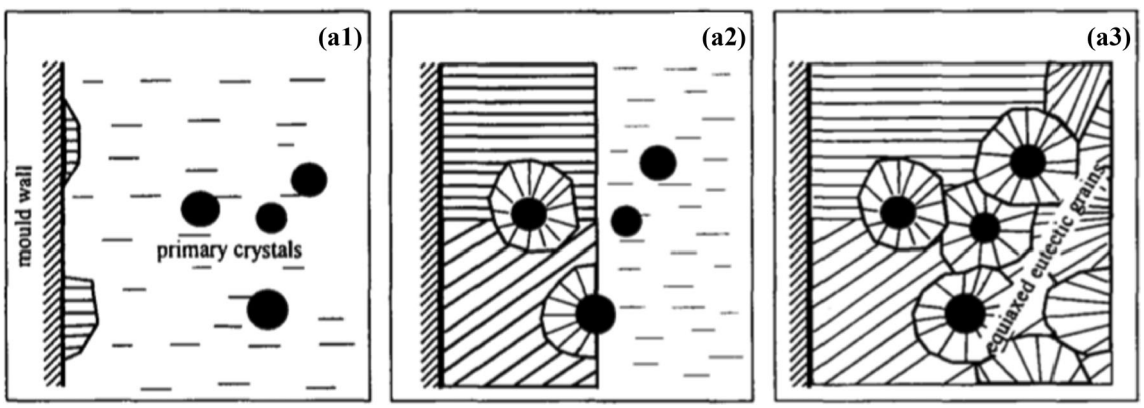

Figure 20 Schematic illustration of growth of columnar and equiaxed regions in casting of hypereutectic alloy for the cases **a1** Initial growth stage of primary and secondary phase, **a2** Grain growth if primary phase is not the leading phase, **a3** Grain growth if primary phase is the leading phase. Adapted with permission from reference [43]. Copyright 1996, Taylor & Francis.

columnar grains nucleated on the mould walls. In addition, high pouring temperature can also dissolve any pre-existing nuclei, which form when the melt is poured into the mould. This leads to growth of grains, which are attached to the mould wall in a columnar structure as in Fig. 21a. At low pouring temperatures, the pre-existing nuclei formed are hard to be dissolved into the melt due to insufficient heat. This leads to simultaneous nucleation and growth in the centre and along the mould wall. Hence, they observed the formation of equiaxed grains in the centre of the casting while a columnar structure near the mould wall as in Fig. 21b [43]

Another evidence supporting this theory was obtained by Huang., Xing, and Guo [69] who experimented with slope cooling method, in which the melt of a HCCI was poured into the sand mould via an inclined slope cooling body with BN coating. The coating allowed easy dissociation of primary carbide nuclei. It was observed that decreasing the pouring temperature led to increase in number of primary carbide nuclei. The nuclei formed on the slope and were dissociated quickly and easily because of coating and flowing melt, hence hindering their growth [69]. This method did produce shrinkage porosity in the casting but led to change in morphology and improvement in mechanical properties by refining the primary carbides [44, 69].

Both the Free Chill Crystal theory and Separation theory emphasize on the formation of primary crystals on the mould wall and breaking away due to either solute rejection or mechanical or thermal fluctuations. It has been observed that relatively refined microstructure is obtained at low pouring temperatures [43]. At such temperatures, the convection in the melt is not enough to transport the primary carbide nuclei to the centre of the casting. Nevertheless, the primary carbides are evenly refined in the whole casting. Hence, in terms of mechanism of refinement of primary carbides in Fe–Cr–C alloy system, there is a need for detailed investigation to understand the process of refinement.

Peritectic reaction based theories

These theories were based on the fact that addition of titanium into aluminium and its alloys and addition of Zr into Al/Mn/Si-free magnesium and its alloys lead to significant grain refinement of the cast alloys. As both Al–Ti and Mg–Zr are peritectic systems, it was considered that a peritectic reaction is responsible for the grain refinement in cast aluminium and magnesium alloys. For both systems, master alloys are commercially available to add Ti and Zr. In aluminium alloys, the peritectic reaction occurs between liquid aluminium and Al_3Ti, leading to the formation of α-Al. For Al/Mn/Si free magnesium alloys, the peritectic reaction occurs between liquid magnesium and α-Zr, leading to the formation of α-Mg [104, 168, 189].

In cast aluminium alloys, it was also observed that cooperative addition of Ti and B leads to more significant grain refinement due to the formation of TiB_2 that acts nucleant. Peritectic Hulk theory [190] considers that Al_3Ti is a better nucleant than TiB_2. But, Al_3Ti is not thermally stable in the melt and dissolves

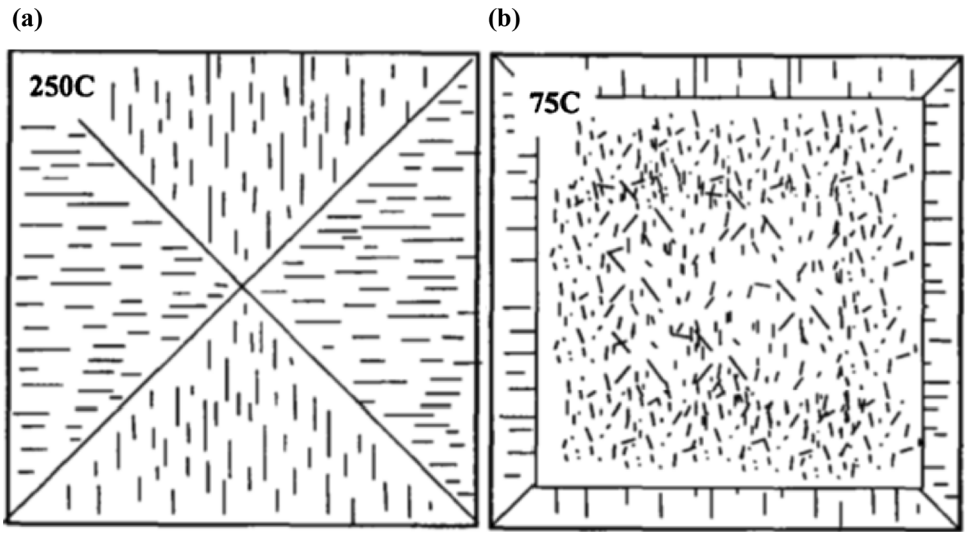

Figure 21 Schematic demonstration of as-cast macrostructure in hypereutectic alloy at **a** high and **b** low pouring temperature. Adapted with permission from reference [43]. Copyright 1996, Taylor & Francis.

in a short time. According to the theory, the boride forms a shell around the aluminide and slows down its dissolution in the aluminium melt. After the peritectic reaction occurs inside the shell, the TiB_2 shell dissolves in the Al [90, 191].

Although this theory explained a few experimental observations, there were still some fundamental limitations with the theory. First, it claims that the boride needs time to dissolve in the melt before they can precipitate on the slowly dissolving Al_3Ti. But, it is hardly possible as Al_3Ti dissolves within minutes at high temperatures [192]. Second, experiments on hypoperitectic aluminium alloys prove that high grain refining efficiency can also be achieved, and thus, peritectic reaction is not essential in grain refinement. Finally, Johnsson, Backerud and Sigworth [191] performed repeated meting and solidification experiments to see if the mechanism for protection of Al_3Ti at nucleation temperature (i.e. peritectic temperature) was active. If the protection mechanism was active, they expected a decrease in nucleation temperature due to repeated cycles as high Ti concentration will be equilibrated. But, they found neither change in nucleation temperature nor in grain size, indicating peritectic reaction is not the grain refinement mechanism. Boride particles acted as a more potent nucleation site in the presence of boron, which is in agreement with the studies which found boride particles at the center of the grains at the hypoperitectic concentration of titanium [90, 104].

Hypernucleation

This theory was put forward by Jones and Pearson [193] owing to the significant grain refining efficiency of small amounts of titanium and boron for aluminium alloys. They calculated the individual activities of the segregating elements such as 0.005% Ti in Al melt at 1050 K and considered that the segregation of Ti atoms at the TiB_2-melt interface forms Al–Ti pseudo crystals which enhance the formation of α-Al at very small undercooling [193]. They also claimed that there is an activity gradient when TiB_2 is introduced into the Al melt. But, this thermodynamically cannot happen because all the activity gradients and chemical potentials are constant at equilibrium [194].

Duplex nucleation

This theory was proposed in 1990′s. Opposite to the Peritectic Hulk theory, this theory considers that a layer of aluminide or Al_3Ti forms over TiB_2 particles, which further acts as nucleation sites for α-Al. This hypothesis was confirmed by Schumacher et al. who found a thin, stable adsorbed layer of Al_3Ti on the 0001 basal faces of the boride, which acted as nucleation site for α-Al [189, 195]. As this theory has been reviewed widely, no more details are included in the present review.

Epitaxial nucleation model

This is the most recent model put forward by Z Fan [196], to understand the mechanism of grain refinement. In the model, it was proposed that heterogenous nucleation of a phase occurs on a potent substrate (S) by epitaxial growth of pseudomorphic solid (PS) layer on the surface of the substrate. Analytically it was proved that critical undercooling and critical thickness for epitaxial nucleation are related to lattice misfit created by the nucleating phase at the PS/S interface to transform pseudomorphic layer to nucleating phase. Fan et al. [197] provided experimental evidence in support of this model by applying it on Al/Al–Ti–B system. However, the application of this model on other multi-component systems is yet to be explored.

Grain growth restriction by solute elements or solute paradigm

The idea of solute paradigm was firstly proposed in 1993, but only gained attraction when previously proposed theories failed to explain the grain refinement due to various irregularities. As specified by the Winegard and Chalmers Theory, segregation of solutes is related to grain refinement of cast metals, light alloys in particular before the concept of growth restriction factor was proposed [101, 198–201]. During solidification of alloys, thermal undercooling is firstly created near the mould walls, depending on the cooling rate. Once the thermal undercooling dissipates, constitutional undercooling (ΔT_c) is generated ahead of the growing solid/liquid interface due to the segregation of solutes in the melt. This constitutional undercooling is necessary to promote the nucleation of new grains within the constitutional

undercooling zone, which further restricts the grain growth [90, 191]. The theory was further developed by taking the rate of development of constitutional undercooling zone into consideration. This is known as growth restriction factor, Q, as represented in Eq. 2 for a binary alloy system [202].

$$Q = mC_o(k-1) \tag{2}$$

where m is the slope of the liquidus line, C_o is the composition of the alloy and k is the partition coefficient. In the absence of interaction of solutes, this parameter Q measures the effect of solute in grain refinement of the alloy [199]. Higher Q-value implies more rapid formation of constitutionally undercooled zone, resulting in smaller grains [101, 198]. For multicomponent systems, the growth restriction factor, Q, is extended based on the initial rate of development of constitutional undercooling with fraction of growing solid phase and is represented as [201].

$$Q = \left(\frac{\partial(\Delta T_{CS})}{\partial f_s}\right)_{f_s \to 0} \tag{3}$$

where $\triangle T_{CS}$ is constitutional undercooling, f_s is fraction of solid. In the most recent work, Fan et al. [203] identified the limitations of Q to effectively quantify the growth restriction effect of different solute elements during alloy solidification. They confirmed via phase field simulations and theoretical analysis that growth velocity is a function of a growth restriction parameter, β for multicomponent systems which incorporates nature of solutes (m and k), solute concentrations (C_o) and solidification conditions such as undercooling (ΔT). It is represented as below

$$\beta = \frac{Q}{\Delta T} - k = \frac{f_L}{f_s} \tag{4}$$

where Q is the growth restriction factor, $\triangle T$ is the undercooling, k is the partition coefficient and f_s and f_L are the fraction of solid and liquid, respectively. However, the authors considered the case of dilute alloys only. Thus, for linear additivity of β in multicomponent systems, the interaction between solutes is either ignored or considered small.

The theory was supported by many experimental evidences across various alloys. Aluminium alloys were refined by Al–Ti–B master alloys with excess Ti, magnesium alloys were refined by Al and SiC additions and titanium alloys were refined by its own native particles along with Si/B/Be as solute additions [90, 172, 181].

The interdependence theory

StJohn et. al proposed this theory in 2011, to understand the mechanism of grain refinement. The theory provides an analytical model that establishes a link between nucleant selection and grain growth to predict the grain size in as-cast structure and the effect of nucleant particle additions [167]. The model assumes that the resultant grain size of the casting is interdependent on nucleation and growth actions, which are governed by the alloy chemistry. As per the theory, the final grain size depends on the three main factors that are as follows and are depicted in Fig. 22.

1. X_{CS}—the minimum distance the previous grain must grow to generate enough constitutional undercooling (CS) that can further lead to nucleation on next potent particles
2. X'_{dl}—the distance known as diffusion length, from the solid–liquid interface at X_{CS} to the point of enough ΔT_{CS} which can lead to nucleation of the next grain
3. X_{SD}—the distance X_{nfz} to the point where the next nucleation event can occur

Mathematically, the interdependence theory is represented as.

$$d_{gs} = X_{CS} + X'_{dl} + X_{SD} \tag{5}$$

where d_{gs} is the calculated grain size of the microstructure. The theory has been applied to predict the as-cast grain size of light metal alloys [204, 205]. The result does provide direction for

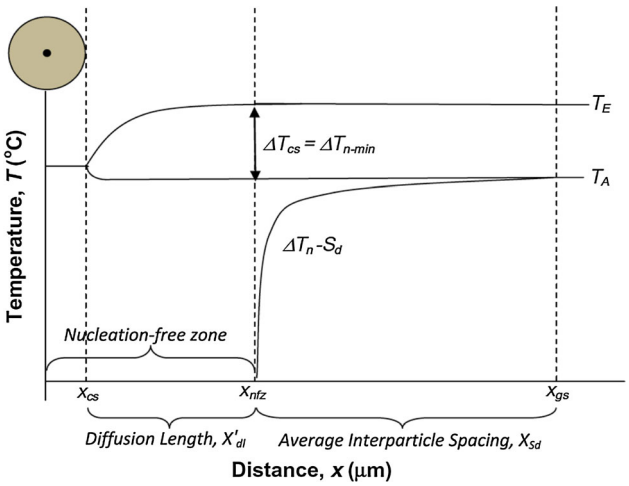

Figure 22 Schematic representation of solidification pathway as proposed by Interdependence theory. Adapted with permission from reference [167]. Copyright 2011, Elsevier.

future work in order to better predict the as-cast grain size. There are a few difficulties to use the theory for grain size prediction. First, the majority of the diffusion and thermodynamic data for multi-component system are not available and the calculation had to be based on the approximation. Thus, the accuracy of the prediction is low. In addition, the theory cannot predict the nucleants and solutes, which can lead to more nucleation and create smaller nucleation free zone (X_{nfz}), for example for primary carbides in HCCIs. Finally, it is also hard to apply the thesis theory to multicomponent systems, such as steels.

Free growth model

Predicting the size of refined grains in the cast alloys has been a major objective for the researchers. In light of this, a numerical model was proposed by Greer et. al [206]. It indicates that the critical undercooling required for heterogeneous nucleation decreases with increase in the size of the nucleant. For a particular undercooling, the smallest nucleant size leading to heterogeneous nucleation is $d \geq 2r^*$, where d is the diameter of the nucleant and r^* is the critical radius of the nucleus [206]. The model considers the nucleating particle as sphere and its diameter is related to undercooling by the equation below.

$$\Delta T_n = \frac{4\sigma_{SL}}{\Delta S_v d_p} \tag{6}$$

where σ_{SL} is the interfacial energy at the solid–liquid interface, ΔS_v is the entropy of fusion per unit volume and d_p is the diameter of the nucleating particle. The model has been successfully applied to aluminium alloys with TiB_2 as inoculant and on magnesium alloys with Zr and SiC as inoculants [207–209]. However, the application of the model is limited by the lack in values of interfacial energy and entropy of fusion for other metals and alloys.

Two-dimensional lattice misfit model

Turnbull and Vonnegut [210] first proposed a crystallographic model in 1952, to assess the suitability of heterogeneous nucleation substrates and their ability to promote growth of precipitating phases. It is based on two assumptions. One is that the nucleating phase forms on a stable heterogeneous substrate, and another is the existence of an interfacial tension equilibrium between the liquid and the heterogeneous substrate.

According to the model, the heterogeneous nucleation depends on crystallographic disregistry between the nucleating phase and the heterogeneous substrate. In other words, the grain refining effectiveness of any substrate is directly proportional to the similarity in the lattice parameter of low index crystallographic planes of nucleating phase and the substrate. This disregistry or misfit is given by the equation below.

$$\delta = \frac{\Delta a_o}{a_o} \tag{7}$$

where δ is the disregistry or the misfit, a_o is the lattice parameter of the nucleating phase and Δa_o is the difference in the values of lattice parameter between the substrate and the nucleating phase. The original equation proposed for calculating disregistry was for linear disregistry only.

In 1970, Bramfitt [159] performed experiments on 20 compounds acting as heterogeneous nucleation substrates in α ferritic iron. He put forth a modified Turnbull–Vonnegut equation for disregistry. The general form of the equation is as below.

$$\delta_{(hkl)_n}^{(hkl)_s} = \sum_{i=1}^{3} \frac{\left| d_{[uvw]_s^i} \cos\theta - d_{[uvw]_n^i} \right|}{d_{[uvw]_n^i}} \times 100\% \tag{8}$$

where δ is the disregistry or the misfit, (hkl) is a low index plane, $[uvw]$ is a low index direction on the (hkl) plane, θ is the angle between a pair of low index directions on low index (hkl) plane and n and s are references to nucleus and inoculant/substrate, respectively. As per modified equation, the criterion for a heterogeneous substrate to be considered effective is when the calculated disregistry is less than 12 per cent.

Over the years, the theory has been widely used to crystallographically evaluate the grain refining efficiency of various particles for different alloys [95, 110, 158, 160, 169, 211, 212]. However, the theory is unable to independently predict the crystallographic relationships between the heterogeneous substrate and the nucleating phase. A major limitation of the theory that it does not specify which index planes and directions need to be selected to calculate disregistry. Due to the difference in selection of low

indices planes and directions, the published results can be contradictory [177].

Edge to edge matching (E2EM) model: a successful case

The model was first coined and developed by MX Zhang and PM Kelly in 1999 [213] to investigate, understand and predict the crystallographic features of diffusional phase transformations in solids. Based on the first principles, the theory of the model takes two assumptions into account. First, the morphology and orientation relationships between the matrix and the precipitate are based on minimization of energy at their interface. Second, the energy minimization can be achieved through maximization of the atomic matching across the interface between the matrix and the precipitate. As shown in Fig. 23, in order to maximize the atomic matching, the model requires the directions with rows of atoms which are close packed or nearly close packed in both the phases should match with each other with low interatomic mismatching between the two phases. The planes containing these matching directions should be close packed or nearly close packed and are associated with compatible interplanar spacing between the matrix and the precipitates. Based on the matching directions and the matching planes, crystallographic features, including orientation relationships and habit planes can be predicted for any two crystals. The E2EM model can be considered as more reliable because it is based on the first principles and is valid for most common situations i.e. semi-coherent precipitates which are widely observed across both ferrous and non-ferrous alloys. This model not only predicts the already published and most common orientation relationships but also has consistently predicted the new orientation relationships of any systems [213]. The model has been successfully applied on light metal alloys, and it has not only been used for explaining the grain refinement but also in the identification of grain refiners [170, 214, 215].

The application of the E2EM model to grain refinement can be done through consideration of the crystallographic features between the heterogeneous nucleation substrate or nucleant and the nucleating phase. The grain refinement efficiency is related to the interatomic misfit along the matching directions and to the interplanar spacing mismatching between the matching planes. Lower misfit and mismatch correspond to high refining potency of the inoculant for a particular alloy system. Thus, the model has been not only successful in developing new grain refiners for various cast metals [163, 216–218], but also been able to predict the order of grain refining potency of the inoculants for a particular alloy system [219, 220]. Hence, this model has high potential to be used to exploit new and more effective modifiers for the primary M_7C_3 carbide in HCCIs.

For comparison purpose, the above-mentioned theories/models of grain refinement are summarized in Table 2.

As stated above, the majority of grain refinement theories/models were developed/established for cast metals, light alloys in particular. Many researchers have worked with light metal alloys, but a very few have studied Fe–Cr–C system. Particularly, in the case of hypereutectic high-chromium cast irons, the mechanism of refinement of primary carbides needs more investigation. This is because the mechanism will help us correlate the addition of nucleant or solute or any other method with changing size, shape and distribution of primary carbides. The better control over the microstructure will lead to better understanding of variation of mechanical properties with change in microstructure. Except for the ECP, there is still lack of valid theories/models to understand the carbide refinement in HCCIs. The question

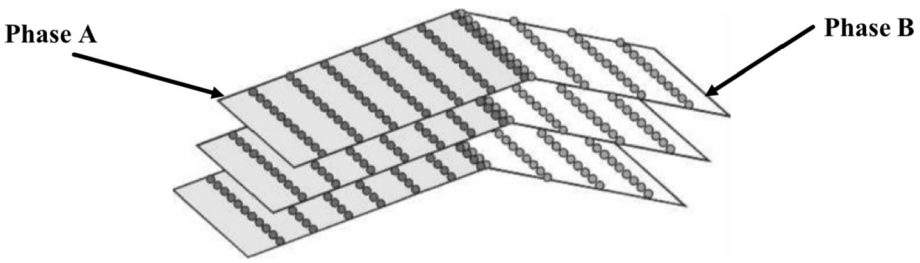

Figure 23 Schematic illustration of matching of two close-packed atoms rows and two close packed planes in two phases under E2EM model. Adapted with permission from reference [219]. Copyright 2006, Springer Nature.

Table 2 Summary of theories/models of grain refinement developed for cast metals

Alloy system	Theory/Model	Nucleant	Rational
All alloys systems	Winegard and Chalmers theory	Inclusions, ceramic particles, such as borides and carbides	Solutes rejected at the solid–liquid interface create constitutional undercooling, paving way for heterogenous nucleation
	Free chill crystal theory	Chill crystals segment	Chill crystals nucleated on the mould wall get detached due to rejection of solute and heat conduction, move into the melt by convection and grow into equiaxed crystals
	Separation theory	Mould wall for pure metals, Primary or eutectic leading phase for alloys	For pure metals, crystals nucleate on mould wall and continue to grow until they meet adjacent crystals. No equiaxed crystals form For alloys, if primary phase is the leading phase, primary phase forms on the mould wall, gets detached, moves towards centre via convection and forms equiaxed crystals. If primary phase is not the leading phase, columnar crystals are formed
Aluminium alloys	Peritectic reaction-based theories	Pro-peritectic phase	Grain refinement is achieved by peritectic reaction
	Hypernucleation	Boride particles	TiB_2 forms on the surface of Al_3Ti particle to prevent the Al_3Ti from dissolving
	Duplex nucleation	Al_3Ti formed over TiB_2 particles	Ti segregates to form Al_3Ti over TiB_2 particles which acts as a nucleant for α-Al
Aluminium, Magnesium alloys	Interdependence theory	Native or any type of nucleants	The integrated description of the effects of solute and heterogeneous nucleation on the grain refinement. Using thermodynamic and diffusion data of the nucleant and solute in the alloy system, the grain size can be predicted
	Free growth model	Native or any type of nucleants	Heterogeneous nucleation prefers to occur on large particles in the melt. To enable the nucleation, the diameter of the nucleant should be over a critical size
	E2EM model	Particles and the nucleating phase are with low interatomic misfit along the matching directions and low interplanar mismatch between the matching plane	Heterogeneous nucleation commonly occurs on particles with minimized interfacial energy, which can be achieved through maximizing the atomic matching between the nucleant and the nucleating phase
Aluminium, Magnesium, Ferrous alloys	2-D Lattice misfit model	Particles and the nucleating phase are with low crystallographic deregistry	Similar to the E2EM model, but it considers that maximum atomic matching can be achieved through lowering the lattice deregistry between the nucleating phase and nucleant

Table 2 continued

Alloy system	Theory/Model	Nucleant	Rational
Aluminium, Magnesium, Titanium alloys	Solute Paradigm (growth restriction factor and growth restriction parameter)	Native nucleant	Solutes in the melt lead to the establishment of a constitutional undercooling (CS) zone at front of the growing solid–liquid interface. Nucleation within this CS zone suppresses the further growth of the solid. Growth restriction factor is related to the establishment rate of the CS zone and the growth restriction parameter is associated with relative fraction of the solid and liquid

that arises is whether the current grain refinement theories/models for cast metals can be used to understand the refinement mechanism of the primary carbide and how to develop new techniques to further modify/refine the carbide in various HCCIs.

Possibilities to apply the current theories/models of grain refinement for cast metals to modification of primary carbide in HCCIs

Although grain refinement for cast metals has been studied in-depth due to its importance, the modification of primary carbide in HCCIs is still based on trial and error approach. According to the present review, it can be seen that the solidification process of HCCIs is very similar to that of light alloys. In hypereutectic HCCIs, it is the primary M_7C_3 carbide directly forms from the liquid, whereas in light alloys, they are α-Al or α-Mg. Hence, the theories/models of grain refinement developed in light alloys have strong potency to be used to develop new and more effective modifiers for HCCIs. In fact, the current electrical pulse process and dynamic solidification process discussed in "Modification of primary carbides in high-chromium cast irons through process control" section were based on the Free Chill Crystal theory and Separation theory. However, in order to fully comprehend the modification of primary carbide, the challenge to understand its mechanism needs to be addressed. There are a few challenges to use the current theories/models of grain refinement to hypereutectic HCCIs.

First, most HCCIs are multi-component systems with a large number of solutes, which affect the solidification individually and via solute–solute interactions. Particularly for the case of hypereutectic high-chromium cast irons, the formation of phases depends hugely on C and Cr contents. Second, there is lack of M_7C_3-based phase diagrams and/or thermodynamic data, which makes difficulty to calculate the growth restriction factor and growth restriction parameter and to obtain data to prediction the grain size. Hence, neither the Solute Paradigm nor the Interdependent Theory can be directly used. Finally, the crystal structure of M_7C_3 carbide is more complicated than both α-Al and α-Mg. The low indexed planes and directions are not typical. Thus, the 2D lattice misfit model is invalid. In terms of this analysis, the present authors consider that the only theory/model can be used is the E2EM model to identify potential modifiers for the carbide and the Free Growth Theory to specify the particle size to be used.

Summary

In spite of being used for decades, hypereutectic high-chromium cast irons with high abrasion resistance and hardness have been suffered from low toughness, and therefore low service life. Because the coarse hexagonal primary M_7C_3 carbide is responsible for the low toughness, modification of such primary carbides has been critical in production of HCCI engineering components. Although there are various techniques available to control the morphology of the carbide during casting, they all have

limitations. For example, the processing control methods are restricted by the size of castings and by the cast methods; the solute addition approaches cold lead to variation of the feature of the HCCIs from hypereutectic to hypoeutectic, which lowers its wear resistance; and the efficiency of the currently available modifiers, such as TiC and TiBAl, is not satisfied. In addition, there has also been lack of fundamental study to understand the mechanisms of carbide modification in HCCIs. In order to improve the properties, toughness in particular, of the HCCIs, and therefore to increase their service life, two challenges need to be addressed. One is to discover and develop new and more effective modifiers to convert the needle morphology into equiaxed and to refine carbide. Another is to investigate and understand the fundamental mechanism, which governs the size, shape and distribution of the refined primary carbides. Due to the similarity of solidification process of HCCIs to light metals, it is proposed to apply the available grain refinement theories/models developed in light metal, the E2EM model and Free Growth Model in particular, to develop new and more effective modifiers for hypereutectic HCCIs and to understand its mechanisms.

Acknowledgements

The authors would like to thank Australia Research Council (ARC) Industrial Transformation Training Centre program (IC160100036) for funding support.

Compliance with ethical standards

Conflict of interest The authors declare that they have no conflict of interest.

References

[1] Read JA (1970) The effects of aluminum and manganese on the structure and properties of cast iron

[2] George L, Richard G, Klaus R (2000) Abrasion-resistant cast iron handbook. American Foundry Society, Illinois

[3] Sare IR, Arnold BK (1995) The effect of heat treatment on the gouging abrasion resistance of alloy white cast irons. Metall Mater Trans A 1995(26A):357–370

[4] K.H. Andrews, A.R.M.I.T., M.I.B.F (1972) Cast Wear-Resistant Materials for the Mining Industry. Inst. British Foundrymen, Australian Branch, 23:75–93.

[5] Liu H-N, Sakamoto M, Nomura M, Ogi K (2001) Abrasion resistance of high Cr cast irons at an elevated temperature. Wear 250:71–75

[6] Powell GLF, Laird II G (1992) Structure, nucleation, growth and morphology of secondary carbides in high chromium and Cr-Ni white cast irons. J Mater Sci 27:29–35. https://doi.org/10.1007/BF00553833

[7] Porter DA, Easterling KE (2009) Phase transformations in metals and alloys (revised reprint). CRC press

[8] Tabrett CP, Sare IR, Ghomashchi MR (1996) Microstructure-property relationships in high chromium white iron alloys. Int Mater Rev 41:59–82

[9] Anon, Cast Iron- A review of recent developments. Eng Mater Des, 1978. **22**(3): 60–65.

[10] Becket FM (1916) Alloy. Electro Metallurgical Co, US

[11] Zum Gahr KH, Scholz WG (1980) Fracture toughness of white cast irons. J Metals 32:38–44

[12] Wiengmoon A et al (2005) Microstructural and crystallographical study of carbides in 30wt.%Cr cast irons. Acta Mater 53(15):4143–4154. https://doi.org/10.1016/j.actamat.2005.05.019

[13] Coronado JJ (2011) Effect of $(Fe, Cr)_7C_3$ carbide orientation on abrasion wear resistance and fracture toughness. Wear 270(3–4):287–293. https://doi.org/10.1016/j.wear.2010.10.070

[14] Filipovic M, Romhanji E, Kamberovic Z (2012) Chemical composition and morphology of M_7C_3 eutectic carbide in high chromium white cast iron alloyed with vanadium. ISIJ Int 52(12):2200–2204. https://doi.org/10.2355/isijinternational.52.2200

[15] Tabrett CP, Sare IR (2000) Fracture toughness of high-chromium white irons- Influence of cast structure. J Mater Sci 35:2069–2077. https://doi.org/10.1023/A:1004755511214

[16] Lu L, Soda H, McLean A (2003) Microstructure and mechanical properties of Fe-Cr-C eutectic composites. Mater Sci Eng A 347:214–222

[17] Hongsug OH, Lee S, Jung J-Y, Ahn S (2001) Correlation of microstructure with the wear resistance and fracture toughness of duocast materials composed of high-chromium white cast iron and low-chromium steel. Metall Mater Trans A 32A:515–524

[18] Adachi Y, Hakata K, Tsuzaki K (2005) Crystallographic analysis of grain boundary Bcc-precipitates in a Ni–Cr alloy by FESEM/EBSD and TEM/Kikuchi line methods. Mater Sci Eng A 412(1–2):252–263. https://doi.org/10.1016/j.msea.2005.09.033

[19] Laird G, Nielsen RL, MacMillan NH (1991) On the nature of eutectic carbides in Cr-Ni white cast irons. Metall Trans A 22A:1709–1719

[20] Neville A, Reza F, Chiovelli S, Revega T (2006) Characterization and corrosion behavior of high-chromium white cast irons. Metall Mater Trans A 37A:2339–2347

[21] Maratray FF (1971) Choice of appropriate compositions for chromium-molybdenum white irons. Trans Am Foundrymen's Soc 79:121–124

[22] Standard AS. E963 (2010) Standard practice for electrolytic extraction of phases from Ni and Ni-Fe base superalloys using a hydrochloric-methanol electrolyte. ASTM International, West Conshohocken

[23] Xu ML (2012), Secondary carbide dissolution and coarsening in 13% Cr martensitic stainless steel during austenitizing. In: Department of Mechanical and Industrial Engineering. Northeastern Univeristy, Boston, Massachusetts.

[24] Dogan ÖN, Hawk JA, Laird II G (1997) Solidification structure and abrasion resistance of high chromium white irons. Metall Mater Trans A 28A:1315–1328

[25] Kitaigora NI (1975) Impact-abrasion wear resistance of high-chromium cast iron. Met Sci Heat Treat 17(5–6):417–420

[26] Hebbar BM, Seshan S (1994) Fracture toughness of high-chromium cast irons. In: AFS Transactions pp. 349–356

[27] Adler TA, Dogan ON (2002) Erosive wear and impact damage of high-Cr white cast irons. AFS Transactions 110:495–500

[28] Adler TA, Dogan ON (1999) Erosive wear and impact damage of high-chromium white cast irons. Wear 225–229:174–180

[29] Magnée A (1995) Generalised law of erosion: application to various alloys and intermetallics. Wear 181:500–510

[30] ASTM International. E604-18 (2018) Standard test method for dynamic tear testing of metallic materials. ASTM International, West Conshohocken, PA. https://doi.org/10.1520/E0604-18

[31] Fulcher JK, Kosel TH, Fiore NF (1983) The effect of carbide volume fraction on the low stress abrasion resistance of high Cr-Mo white cast irons. Wear 84:313–325

[32] Svensson LE, Gretoft B, Ulander B, Bhadeshia HKDH (1986) Fe-Cr-C hardfacing alloys for high-temperature applications. J Mater Sci 21:1015–1019. https://doi.org/10.1007/BF01117388

[33] Atamert S, Bhadeshia HKDH (1990) Silicon modification of iron base hardfacing alloys. In: David A, Vitek JM (eds) Recent trends in welding science and technology (TWR'89). Materials Park, Ohio, pp 273–278

[34] Norman TE (1985) Abrasion resistant refrigeration hardenable ferrous alloys. US4547221A

[35] Hornung J, Zikin A, Pichelbauer K, Kalin M, Kirchgaßner M (2013) Influence of cooling speed on the microstructure and wear behaviour of hypereutectic Fe–Cr–C hardfacings. Mater Sci Eng A 576:243–251. https://doi.org/10.1016/j.msea.2013.04.029

[36] Lei TS, Chang WS, Dong SY (2006) The effect of fluid convection on microstructures of directionally solidified castings. Mater Sci Forum 508:473–478. https://doi.org/10.4028/www.scientific.net/MSF.508.473

[37] Laird II G (1991) Microstructures of Ni-hard I Ni-hard IV and high-Cr white cast irons. AFS Trans 99:339–357

[38] Laird II G (1993) Some comments on white cast iron microstructures and wear properties. AFS Trans 101:497–504

[39] Yang DS et al (2014) The effect of directionally chilled microstructure on hypereutectic high-chromium white cast iron. Adv Mater Res 912–914:399–403. https://doi.org/10.4028/www.scientific.net/AMR.912-914.399

[40] Yang D-S, Lei T-S (2012) Investigating the influence of mid-chilling on microstructural development of high-chromium cast iron. Mater Manuf Process 27(9):919–924. https://doi.org/10.1080/10426914.2011.602793

[41] Zhi XH et al (2013) Effect of fluctuation, modification and surface chill on structure of 20%Cr hypereutectic white cast iron. Mater Sci Technol 25(1):56–60. https://doi.org/10.1179/174328407x245139

[42] Liu Q et al (2012) Effect of cooling rate and Ti addition on the microstructure and mechanical properties in as-cast condition of hypereutectic high chromium cast irons. ISIJ Int 52(12):2210–2219. https://doi.org/10.2355/isijinternational.52.2210

[43] Laird G, Doğan ÖN (1996) Solidification structure versus hardness and impact toughness in high-chromium white cast irons. Int J Cast Met Res 9(2):83–102. https://doi.org/10.1080/13640461.1996.11819648

[44] Huang Z, Xing J, Zhang A (2006) Investigation of microstructure and impact toughness of semisolid hypereutectic high chromium cast iron prepared by slope cooling body method. J Appl Sci 6:1635–1640

[45] Powell GLF, Carlson RA, Randle V (1994) The morphology and microtexture of M_7C_3 carbides in Fe-Cr-C and Fe-Cr-C-Si alloys of near eutectic composition. J Mater Sci 29:4889–4896. https://doi.org/10.1007/BF00356539

[46] Chen H et al (2012) Effect of electric current pulse on carbide in hypereutectic high chromium cast iron. Adv Mater Res 457–458:174–180. https://doi.org/10.4028/www.scientific.net/AMR.457-458.174

[47] Geng B et al (2018) Change in primary (Cr, Fe)(7)C(3) carbides induced by electric current pulse modification of hypereutectic high chromium cast iron melt. Materials (Basel). https://doi.org/10.3390/ma12010032

[48] Räbiger D et al (2014) The relevance of melt convection to grain refinement in Al–Si alloys solidified under the impact of electric currents. Acta Mater 79:327–338. https://doi.org/10.1016/j.actamat.2014.07.037

[49] Zhang Y et al (2016) Comparative study on the grain refinement of Al-Si alloy solidified under the impact of pulsed electric current and travelling magnetic field. Metals. https://doi.org/10.3390/met6070170

[50] Zhou RF, Jiang YH, Zhou R, Zhang L (2014) Effect of Electric Current Pulse on Solidification Microstructure of Hypereutectic High Chromium Cast Iron Cooling from the Temperature between Liquidus and Solidus.

[51] Lv H, Zhou R, Li L, Ni H, Zhu J, Feng T (2018) Effect of electric current pulse on microstructure and corrosion resistance of hypereutectic high chromium cast iron. Materials 11(11):2220. https://doi.org/10.3390/ma11112220

[52] Zhang Z et al (2008) The cluster size transformation model of molten alloy under pulse electric field. Sci China Ser E Technol Sci 51(3):302–307. https://doi.org/10.1007/s11431-008-0017-9

[53] Qi J et al (2011) An investigation for structure transformation in electric pulse modified liquid aluminum. Phys B Condens Matter 406(4):846–849. https://doi.org/10.1016/j.physb.2010.12.010

[54] Wang J-Z et al (2013) Effects of electric pulse modification on liquid structure of Al–5%Cu alloy. Trans Nonferrous Met Soc China 23(9):2792–2796. https://doi.org/10.1016/s1003-6326(13)62799-5

[55] Conrad H, Sprecher AF, Cao WD, Lu XP (1990) Electroplasticity—the effect of electricity on the mechanical properties of metals. J Metals 42:28–33

[56] Conrad H (2000) Influence of an electric or magnetic field on the liquid—solid transformation in materials and on the microstructure of the solid. Mater Sci Eng A 287:205–212

[57] Nakada M, Shiohara Y, Flemings MC (1990) Modification of solidification structures by pulse electric discharging. ISIJ Int 30:27–33

[58] Spencer DB, Mehrabian R, Flemings MC (1972) Rheological behavior of Sn-15 Pct Pb in the crystallization range. Metall Trans 3:1925–1932

[59] Appendino P, Crivellone G, Mus C, Spriano S (2002) Dynamic solidification of sand-cast aluminium alloys. Metall Sci Technol 20:27–32

[60] Deshpande J (2006), The Effect of Mechanical Mold Vibration on the Characteristics of Aluminium Alloys. Worcester Polytechnic Institute.

[61] StJohn DH, Dahle AK, Abbott T, Nave MD, Qian M (2003) Solidification of cast magnesium alloys. TMS (The Minerals, Metals & Materials Society) 2003:95–100

[62] Pillai RM, Biju Kumar KS, Pai BC (2004) A simple inexpensive technique for enhancing density and mechanical properties of Al–Si alloys. J Mater Process Technol 146(3):338–348. https://doi.org/10.1016/j.jmatprotec.2003.11.022

[63] Gittus JH (1959) The inoculation of solidifying iron and steel castings by means of vibration. J Iron Steel Inst 192:118–131

[64] Nofal A et al (2010) Structural refinement of 15%Cr-2%Mo white irons. Key Eng Mater 457:231–236. https://doi.org/10.4028/www.scientific.net/KEM.457.231

[65] Reda R, Nofal A, Ibrahim K, Hussien A (2010) Investigation of improving wear performance of hypereutectic 15%Cr-2%Mo white irons. China Foundry 7(4):438–446

[66] Kantenik SN, Karpenko MI, Svyatkin BK, Spasskii KV (1974) Influence of ultra-sound and inoculation on the graphitization process of malleable iron. Izvestiya VUZ Chernaya Metall 7:143–147

[67] S.K. Kantenik, M.I.K., B.K. Svyatkin, Ultrasonic degassing of iron melts. Russian Castings Production, (7): p. 284–285.

[68] Huang ZF, Xing JD, Gao YM, Cheng XL (2011) Microstructure and properties of hypereutectic high chromium white cast iron prepared under pressure. Ironmak Steelmaking 38(5):359–362. https://doi.org/10.1179/030192310x12706364542821

[69] Huang ZF, Xing JD, Guo C (2013) Microstructure and properties of semisolid hypereutectic high chromium cast iron prepared by slope cooling body method. Ironmak Steelmaking 37(8):607–611. https://doi.org/10.1179/030192309x12549935902266

[70] Kim CK, Lee S, Jung J-Y (2006) Effects of heat treatment on wear resistance and fracture toughness of duo-cast materials composed of high-chromium white cast iron and low-chromium steel. Metall Mater Trans A 37A:633–643

[71] Hinckley B, Dolman KF, Wuhrer R, Yeung W, Ray A (2008) SEM investigation of heat treated high-chromium cast irons. Mater Forum 32:55–71

[72] Dupin P, Saverna J, Schissler JM (1982) A structural study of chromium white cast irons. Trans Am Foundrymen's Soc 90:711–718

[73] Skoblo TS, Vishnyakova EN, Mozharova NM, Dubrov VA, Bondin RD (1990) Increasing the quality of rolling rolls of high-chromium cast iron by high-temperature heat treatment. Metal Sci Heat Treat 32(10):734–736

[74] Pearce JTH (1983) Examination of M_7C_3 carbides in high chromium cast irons using thin foil transmission electron microscopy. J Mater Sci Lett 2:428–432

[75] Zhang MX, Kelly P, Gates JD (2001) The effect of heat treatment on the toughness, hardness and microstructure of

low carbon white cast irons. J Mater Sci 36:3865–3875. https://doi.org/10.1023/A:1017949600733

[76] Zhi X et al (2008) Effect of heat treatment on microstructure and mechanical properties of a Ti-bearing hypereutectic high chromium white cast iron. Mater Sci Eng A 487(1–2):171–179. https://doi.org/10.1016/j.msea.2007.10.009

[77] Yilmaz SO, Teker T (2016) Effect of TiBAl inoculation and heat treatment on microstructure and mechanical properties of hypereutectic high chromium white cast iron. J Alloy Compd 672:324–331. https://doi.org/10.1016/j.jallcom.2016.02.125

[78] Liu Q et al (2012) Effect of heat treatment on microstructure and mechanical properties of Ti-alloyed hypereutectic high chromium cast iron. ISIJ Int 52(12):2288–2294. https://doi.org/10.2355/isijinternational.52.2288

[79] Arnold BK, Sare IR (1995) The influence of heat treatment on the high-stress abrasion resistance and fracture toughness of alloy white cast irons. Metall Mater Trans A 26A:1785–1793

[80] Gasan H, Erturk F (2013) Effects of a destabilization heat treatment on the microstructure and abrasive wear behavior of high-chromium white cast iron investigated using different characterization techniques. Metall Mater Trans A 44(11):4993–5005. https://doi.org/10.1007/s11661-013-1851-3

[81] Abdel-Aziz K, El-Shennawy M, Omar AA (2017) Microstructural characteristics and mechanical properties of heat treated high-Cr white cast iron alloys. Int J Appl Eng 12:4675–4686

[82] Hinckley B, Dolman KF, Wuhrer R, Ray A, Yeung W (2008) SEM and EBSD investigations of high-chromium cast irons. Microsc Microanal 14(S2):550–551. https://doi.org/10.1017/s1431927608084067

[83] Powell GLF (1980) Morphology of eutectic M_3C and M_7C_3 in white iron castings. Metals Forum 3(1):37–46

[84] Inthidech S, Sricharoenchai P, Matsubara Y (2006) Effect of alloying elements on heat treatment behavior of hypoeutectic high chromium cast iron. Mater Trans 47:72–81

[85] Inthidech S et al (2010) Effect of repeated tempering on hardness and retained austenite of high chromium cast iron containing molybdenum. Mater Trans 51(7):1264–1271. https://doi.org/10.2320/matertrans.M2010018

[86] Bedolla-Jacuinde A, Arias L, Hernández B (2003) Kinetics of secondary carbides precipitation in a high-chromium white iron. J Mater Eng Perform 12(4):371–382

[87] Tabrett CP, Sare IR (1998) Effect of high temperature and sub-ambient treatments on the matrix structure and abrasion resistance of a high-chromium white iron. Scripta Mater 38:1747–1753

[88] Laird G, Powell GLF (1993) Solidification and solid-state transformation mechanisms in si alloyed high-chromium white cast irons. Metall Trans A 24A:981–988

[89] Bunin KP, Taran YN (1967) Metallography of cast iron. Metal Sci Heat Treat 9(5):397–402

[90] Easton M, StJohn D (1999) Grain refinement of aluminum alloys-part I. the nucleant and solute paradigms—a review of the literature. Metall Mater Trans A 30A:1613–1623

[91] Easton M, StJohn D (1999) Grain refinement of aluminum alloys- Part II. confirmation of, and a mechanism for, the solute paradigm. Metall Mater Trans A 30A:1625–1633

[92] Lekakh SN, Neroslavskii OM, Rozum VA (1989) Reaction of complex modifiers with liquid cast iron. Izvestiya Akademii Nauk SSSR Metally 5:12–18

[93] Fu H-G, Wu XJ, Li XY, Xing JD, Lei YP, Zhi XH (2009) Effect of TiC particle additions on structure and properties of hypereutectic high chromium cast iron. J Mater Eng Perform 18(8):1109–1115. https://doi.org/10.1007/s11665-008-9330-5

[94] Roman Radon RR (2016) Hypereutectic white iron alloys comprising chromium and nitrogen and articles made therefrom

[95] Zhi X, Liu J, Xing J, Ma S (2014) Effect of cerium modification on microstructure and properties of hypereutectic high chromium cast iron. Mater Sci Eng A 603:98–103. https://doi.org/10.1016/j.msea.2014.02.080

[96] Chao Chang W, Tsun HH, Qian M (2013) Formation of spheroidal carbide in vanadium white cast iron by rare earth modification. Mater Sci Technol 6(9):905–910. https://doi.org/10.1179/mst.1990.6.9.905

[97] Kopyciński D, Piasny S (2016) Influence of inoculation on structure of chromium cast iron. Characterization of Minerals, Metals and Materials, TMS, 2016

[98] Kopyciński D (2009) Inoculation of chromium white cast iron. Arch Foundry Eng 9(1):191–194

[99] Chung RJ et al (2009) Effects of titanium addition on microstructure and wear resistance of hypereutectic high chromium cast iron Fe–25wt.%Cr–4wt.%C. Wear 267(1–4):356–361. https://doi.org/10.1016/j.wear.2008.12.061

[100] Ali Y et al (2015) Current research progress in grain refinement of cast magnesium alloys: A review article. J Alloy Compd 619:639–651. https://doi.org/10.1016/j.jallcom.2014.09.061

[101] StJohn DH, Qian M, Easton MA, Cao P, Hildebrand Z (2005) Grain refinement of magnesium alloys. Metall Mater Trans 36(7):1669–1679

[102] McCartney DG (1989) Grain refining of aluminium and its alloys using inoculants. Int Mater Rev 34(1):247–260.

[103] Murty BS, Kori SA, Chakraborty M (2013) Grain refinement of aluminium and its alloys by heterogeneous nucleation and alloying. Int Mater Rev 47(1):3–29. https://doi.org/10.1179/095066001225001049

[104] Liu Z (2017) Review of grain refinement of cast metals through inoculation: theories and developments. Metall Mater Trans A 48(10):4755–4776. https://doi.org/10.1007/s11661-017-4275-7

[105] Wu X et al (2007) Effect of titanium on the morphology of primary M_7C_3 carbides in hypereutectic high chromium white iron. Mater Sci Eng A 457(1–2):180–185. https://doi.org/10.1016/j.msea.2006.12.006

[106] Huang ZF et al (2014) Effect of Ti addition on morphology and size of primary M_7C_3 type carbide in hypereutectic high chromium cast iron. Mater Sci Technol 27(1):426–430. https://doi.org/10.1179/026708309x12601952777666

[107] Huang Z, Xing J, Gao Y, Zhi X (2012) Effect of titanium on the as-cast microstructure and impact toughness of hypereutectic high-chromium cast iron. Int J Mater Res 103(5):609–612

[108] Zhang Y et al (2020) The formation of TiC–NbC core-shell structure in hypereutectic high chromium cast iron leads to significant refinement of primary M_7C_3. J Alloys Compd. https://doi.org/10.1016/j.jallcom.2020.153806

[109] Ding H et al (2016) Improving impact toughness of a high chromium cast iron regarding joint additive of nitrogen and titanium. Mater Des 90:958–968. https://doi.org/10.1016/j.matdes.2015.11.055

[110] Wang Y, Zeng X, Ding W (2006) Effect of Al–4Ti–5B master alloy on the grain refinement of AZ31 magnesium alloy. Scripta Mater 54(2):269–273. https://doi.org/10.1016/j.scriptamat.2005.09.022

[111] Davies IG, Dennis JM, Hellawell A (1970) The nucleation of aluminum grains in alloys of aluminum with titanium and boron. Metall Trans 1:275–280

[112] Kopyciński D (2013) The inoculation of white cast iron. In: TMS2013 Annual Meeting Supplemental Proceedings, pp. 601–608.

[113] Studnicki A, Jezierski J (2012) Stereological parameters of carbides in modified wear resistant Fe-C-Cr alloys. In: METAL 2012 - Conference Proceedings, 21st International Conference on Metallurgy and Materials 201, pp. 795–802.

[114] Hao F et al (2011) Effect of rare earth oxides on the morphology of carbides in hardfacing metal of high chromium cast iron. J Rare Earths 29(2):168–172. https://doi.org/10.1016/s1002-0721(10)60425-5

[115] Hao F et al (2011) Effects of rare earth oxide on hardfacing metal microstructure of medium carbon steel and its refinement mechanism. J Rare Earths 29(6):609–613. https://doi.org/10.1016/s1002-0721(10)60507-8

[116] Yang J et al (2014) Microstructure and wear resistance of the hypereutectic Fe–Cr–C alloy hardfacing metals with different La_2O_3 additives. Appl Surf Sci 289:437–444. https://doi.org/10.1016/j.apsusc.2013.10.186

[117] Zhou Y et al (2012) Influence of La_2O_3 addition on microstructure and wear resistance of Fe–Cr–C cladding formed by arc surface welding. J Rare Earths 30(10):1069–1074. https://doi.org/10.1016/s1002-0721(12)60180-x

[118] Tuttle R (2013) Effect of rare earth oxides in plain carbon steels. In: AISTECH: iron and steel technology conference proceedings, vol. **1,** pp. 1085–1093.

[119] Zhi X et al (2008) Effect of titanium on the as-cast microstructure of hypereutectic high chromium cast iron. Mater Charact 59(9):1221–1226. https://doi.org/10.1016/j.matchar.2007.10.010

[120] Bedolla-Jacuinde A et al (2005) Effect of titanium on the as-cast microstructure of a 16%chromium white iron. Mater Sci Eng A 398(1–2):297–308. https://doi.org/10.1016/j.msea.2005.03.072

[121] Kopyciński D et al (2017) The effect of Fe-Ti inoculation on solidification, structure and mechanical properties of high chromium cast iron. Arch Metall Mater 62(4):2183–2187. https://doi.org/10.1515/amm-2017-0321

[122] Kopyciński D, Piasny S (2012) Influence of tungsten and titanium on the structure of chromium cast iron. Arch Foundry Eng 12(1):57–60. https://doi.org/10.2478/v10266-012-0011-3

[123] Filipovic M et al (2013) Microstructure and mechanical properties of Fe–Cr–C–Nb white cast irons. Mater Des 47:41–48. https://doi.org/10.1016/j.matdes.2012.12.034

[124] Wang YP et al (2011) Improving the wear resistance of white cast iron using a new concept—high-entropy microstructure. Wear 271(9–10):1623–1628. https://doi.org/10.1016/j.wear.2010.12.029

[125] Zhi X et al (2008) Effect of niobium on the as-cast microstructure of hypereutectic high chromium cast iron. Mater Lett 62(6–7):857–860. https://doi.org/10.1016/j.matlet.2007.06.084

[126] Maja ME, Maruma MG, Mampuru LA, Moema SJ (2016) Effect of niobium on the solidification structure and properties of hypoeutectic high-chromium white cast irons. J South Afr Inst Min Metall 116(10):981–986. https://doi.org/10.17159/2411-9717/2016/v116n10a14

[127] Liu S et al (2017) Experiments and calculations on refining mechanism of NbC on primary M_7C_3 carbide in

hypereutectic Fe–Cr–C alloy. J Alloy Compd 713:108–118. https://doi.org/10.1016/j.jallcom.2017.04.167

[128] Chen H-X, Chang Z-C, Lu J-C, Lin H-T (1993) Effect of niobium on wear resistance of 15%Cr white cast iron. Wear 166:197–201

[129] Chung RJ et al (2013) Microstructure refinement of hypereutectic high Cr cast irons using hard carbide-forming elements for improved wear resistance. Wear 301(1–2):695–706. https://doi.org/10.1016/j.wear.2013.01.079

[130] Ma Y, Li X, Liu Y, Zhou S, Dang X (2013) Microstructure and properties of Ti–Nb–V–Mo-alloyed high chromium cast iron. Bull Mater Sci 36(5):839–844

[131] Filipovic M, Kamberovic Z, Korac M (2011) Solidification of high chromium white cast iron alloyed with vanadium. Mater Trans 52(3):386–390. https://doi.org/10.2320/matertrans.M2010059

[132] Filipovic M et al (2013) Correlation of microstructure with the wear resistance and fracture toughness of white cast iron alloys. Met Mater Int 19(3):473–481. https://doi.org/10.1007/s12540-013-3013-y

[133] Radulovic M, Fiset M, Peev K, Tomovic M (1994) The influence of vanadium on fracture toughness and abrasion resistance in high chromium white cast irons. J Mater Sci 29:5085–5094. https://doi.org/10.1007/BF01151101

[134] Mampuru LA, Maruma MG, Moema JS (2016) Grain refinement of 25 wt.% high-chromium white cast iron by addition of vanadium. J South Afr Ins Min Metall 116(10):969–972. https://doi.org/10.17159/2411-9717/2016/v116n10a12

[135] M.R. Nikolaenko, G.A.K., N.A. Grinberg, *Influence of boron, vanadium and nickel on the structure and properties of high chromium cast irons deposited with powder-filled strip*. Welding Production, 1973. **20**(4):56–60.

[136] W Zhao, Z Liu, Z Ju, B Liao, X Chen (2008) Effects of vanadium and rare-earth on carbides and properties of high chromium cast iron. Mater Sci Forum 575–578:1414–1419. https://doi.org/10.4028/www.scientific.net/MSF.575-578.1414

[137] Efremenko VG et al (2013) Abrasive wear resistance of spheroidal vanadium carbide cast irons. J Friction Wear 34(6):466–474. https://doi.org/10.3103/s1068366613060068

[138] Bedolla-Jacuinde A et al (2015) Abrasive wear of V-Nb–Ti alloyed high-chromium white irons. Wear 332–333:1006–1011. https://doi.org/10.1016/j.wear.2015.01.049

[139] Zhi X et al (2008) Effect of fluctuation and modification on microstructure and impact toughness of 20 wt.% Cr hypereutectic white cast iron. Materialwiss Werkstofftech 39(6):391–393. https://doi.org/10.1002/mawe.200700219

[140] Shen J, Zhou QD (1988) Solidification behaviour of boron-bearing high-chromium cast iron and the modification mechanism of silicon. Cast Metals 1(2):79–85. https://doi.org/10.1080/09534962.1988.11818951

[141] Jacuinde AB, Rainforth WM (2001) The wear behaviour of high-chromium white cast irons as a function of silicon and Mischmetal content. Wear 250:449–461

[142] Bedolla-Jacuinde A, Rainforth MW, Mejía I (2012) The role of silicon in the solidification of high-Cr cast irons. Metall Mater Trans A 44(2):856–872. https://doi.org/10.1007/s11661-012-1434-8

[143] Powell G, Randle V (1997) The effect of Si on the relationship between orientation and carbide morphology in high chromium white irons. J Mater Sci 32:561–565. https://doi.org/10.1023/A:1018558928916

[144] Jinhai L, Gensheng L, Guolu L, Wang K (1998) Research and application of as-cast wear resistance high chromium cast iron. Chin J Mech Eng 11(2):130–135

[145] Lai J-P et al (2018) Effect of Si content on the microstructure and wear resistance of high chromium cast iron. ISIJ Int 58(8):1532–1537. https://doi.org/10.2355/isijinternational.ISIJINT-2018-099

[146] Inthidech S, Sricharoenchai P, Matsubara Y (2013) Effect of molybdenum content on subcritical heat treatment behaviour of hypoeutectic 16 and 26 wt-% chromium cast irons. Int J Cast Met Res 25(5):257–263. https://doi.org/10.1179/1743133612y.0000000009

[147] Scandian C et al (2009) Effect of molybdenum and chromium contents in sliding wear of high-chromium white cast iron: the relationship between microstructure and wear. Wear 267(1–4):401–408. https://doi.org/10.1016/j.wear.2008.12.095

[148] Kusumoto K et al (2017) Abrasive wear characteristics of Fe-2C-5Cr-5Mo-5W-5Nb multi-component white cast iron. Wear 376–377:22–29. https://doi.org/10.1016/j.wear.2017.01.096

[149] Bereza JM, D.I.T. (1981) Wear and impact resistant white cast irons. The British Foundryman 74(10):205–211.

[150] Yamamoto K, Inthidech S, Sasaguri N, Matsubara Y (2014) Influence of Mo and W on high temperature hardness of M_7C_3 carbide in high chromium white cast iron. Mater Trans 55(4):684–689. https://doi.org/10.2320/matertrans.F-M2014801

[151] Maldonado-Ruíz SI et al (2016) Wear resistance of high chromium—high carbon cast irons. Int J Cast Met Res 15(6):589–594. https://doi.org/10.1080/13640461.2003.11819545

[152] Mousavi Anijdan SH et al (2007) Effects of tungsten on erosion–corrosion behavior of high chromium white cast iron. Mater Sci Eng A 454–455:623–628. https://doi.org/10.1016/j.msea.2006.11.128

[153] Heydari D, Skandani AA, Al Haik M (2012) Effect of carbon content on carbide morphology and mechanical properties of A.R. white cast iron with 10–12% tungsten. Mater Sci Eng A 542:113–126. https://doi.org/10.1016/j.msea.2012.02.040

[154] Lv Y et al (2012) Effect of tungsten on microstructure and properties of high chromium cast iron. Mater Des 39:303–308. https://doi.org/10.1016/j.matdes.2012.02.048

[155] Inoue A, Masumoto T (1994) Light-metal base amorphous alloys containing lanthanide metal. J Alloys Compd 207/208:340–348

[156] Xiao DH et al (2003) Effect of rare earth Ce addition on the microstructure and mechanical properties of an Al–Cu–Mg–Ag alloy. J Alloy Compd 352(1–2):84–88. https://doi.org/10.1016/s0925-8388(02)01162-3

[157] Radulovic M, Fiset M, Peev K (1994) Effect of rare earth elements on microstructure and properties of high chromium white iron. Mater Sci Technol 10(12):1057–1062. https://doi.org/10.1179/mst.1994.10.12.1057

[158] Qu Y et al (2008) Effect of cerium on the as-cast microstructure of a hypereutectic high chromium cast iron. Mater Lett 62(17–18):3024–3027. https://doi.org/10.1016/j.matlet.2008.01.129

[159] Bramfitt BL (1970) The effect of carbide and nitride additions on the heterogeneous nucleation behavior of liquid iron. Metall Trans 1:1987–1995

[160] Zhou YF et al (2012) Fe–24wt.%Cr–4.1wt.%C hardfacing alloy: microstructure and carbide refinement mechanisms with ceria additive. Mater Charact 72:77–86. https://doi.org/10.1016/j.matchar.2012.07.004

[161] Hou Y et al (2012) Influence of rare earth nanoparticles and inoculants on performance and microstructure of high chromium cast iron. J Rare Earths 30(3):283–288. https://doi.org/10.1016/s1002-0721(12)60038-6

[162] Aso S et al (2016) The effect of solidification conditions on phase transformation of iron matrix of Fe-25mass%Cr–C–B alloys. Int J Cast Met Res 11(5):285–290. https://doi.org/10.1080/13640461.1999.11819287

[163] Li M et al (2016) Crystallographic study of grain refinement in low and medium carbon steels. Philos Mag 96(15):1556–1578. https://doi.org/10.1080/14786435.2016.1171413

[164] Li M et al (2017) A new grain refiner for ferritic steels. Metall Mater Trans B 48(6):2902–2912. https://doi.org/10.1007/s11663-017-1101-y

[165] Zhang M et al (2005) Crystallographic study of grain refinement in aluminum alloys using the edge-to-edge matching model. Acta Mater 53(5):1427–1438. https://doi.org/10.1016/j.actamat.2004.11.037

[166] Wang F et al (2013) The grain refinement mechanism of cast aluminium by zirconium. Acta Mater 61(15):5636–5645. https://doi.org/10.1016/j.actamat.2013.05.044

[167] StJohn DH et al (2011) The interdependence theory: the relationship between grain formation and nucleant selection. Acta Mater 59(12):4907–4921. https://doi.org/10.1016/j.actamat.2011.04.035

[168] Crossley FA, Mondolfo LF (1951) Mechanism of grain refinement in aluminum alloys. J Metals 3:1143–1148

[169] Lu L, Dahle AK, StJohn DH (2005) Grain refinement efficiency and mechanism of aluminium carbide in Mg–Al alloys. Scripta Mater 53(5):517–522. https://doi.org/10.1016/j.scriptamat.2005.05.008

[170] Zhang MX et al (2005) Crystallography of grain refinement in Mg–Al based alloys. Acta Mater 53(11):3261–3270. https://doi.org/10.1016/j.actamat.2005.03.030

[171] Men H, Jiang B, Fan Z (2010) Mechanisms of grain refinement by intensive shearing of AZ91 alloy melt. Acta Mater 58(19):6526–6534. https://doi.org/10.1016/j.actamat.2010.08.016

[172] Bermingham MJ et al (2008) The mechanism of grain refinement of titanium by silicon. Scripta Mater 58(12):1050–1053. https://doi.org/10.1016/j.scriptamat.2008.01.041

[173] Tamirisakandala S et al (2005) Grain refinement of cast titanium alloys via trace boron addition. Scripta Mater 53(12):1421–1426. https://doi.org/10.1016/j.scriptamat.2005.08.020

[174] Bermingham MJ et al (2011) Grain-refinement mechanisms in titanium alloys. J Mater Res 23(1):97–104. https://doi.org/10.1557/jmr.2008.0002

[175] Bermingham MJ et al (2011) Segregation and grain refinement in cast titanium alloys. J Mater Res 24(4):1529–1535. https://doi.org/10.1557/jmr.2009.0173

[176] Li M et al (2018) Effect of solutes on grain refinement of As-Cast Fe-4Si Alloy. Metall Mater Trans A 49(6):2235–2247. https://doi.org/10.1007/s11661-018-4571-x

[177] Ji Y, Zhang M-X, Ren H (2018) Roles of lanthanum and cerium in grain refinement of steels during solidification. Metals. https://doi.org/10.3390/met8110884

[178] Winegard WC, Chalmers B (1954) Supercooling and dendritic freezing in alloys. Trans Am Soc Metals 46:1214–1224

[179] Hutt J, Stjohn D (1998) The origins of the equiaxed zone—review of theoretical and experimental work. Int J Cast Met Res 11(1):13–22. https://doi.org/10.1080/13640461.1998.11819254

[180] Cao P, Qian M, StJohn DH (2005) Native grain refinement of magnesium alloys. Scripta Mater 53(7):841–844. https://doi.org/10.1016/j.scriptamat.2005.06.010

[181] Easton MA et al (2006) Grain refinement of Mg–Al(–Mn) alloys by SiC additions. Scripta Mater 55(4):379–382. https://doi.org/10.1016/j.scriptamat.2006.04.014

[182] Liu Y, Liu X, Xiufang B (2004) Grain refinement of Mg–Al alloys with Al_4C_3–SiC/Al master alloy. Mater Lett 58(7–8):1282–1287. https://doi.org/10.1016/j.matlet.2003.09.022

[183] Genders R (1926) The interpretation of the macrostructure of cast metals. J Inst Metal 35

[184] Chalmers BB (1963) The structure of ingots. J Aust Inst Metals 8(3):255–263

[185] Ohno A, Motegi T (1977) Formation mechanism of equiaxed zones in cast metals. AFS Int Cast Metals J 2(1):28–36

[186] Ohno A (1987) Solidification: the separation theory and its practical applications. Springer, New York

[187] Motoyasu G et al (2015) Some perspectives on innovative processing and materials development. J Mater Eng Perform 24(6):2240–2249. https://doi.org/10.1007/s11665-015-1513-2

[188] Ohno A (1996) Grain growth control by solidification technology. Mater Sci Forum 204–206:169–178. https://doi.org/10.4028/www.scientific.net/MSF.204-206.169

[189] Gruzleski JE, Mohantya PS (1995) Mechanism of grain refinement in aluminum. Acta Metall Mater 43:2001–2012

[190] Johnsson M, Bäckerud L (1992) Nucleants in grain refined aluminum after addition of Ti- and B- containing master alloys. Z Metallkd 83(11):774–780

[191] Johnsson M, Bäckerud L, Sigworth GK (1993) Study of the mechanism of grain refinement of aluminum after additions of Ti- and B- containing master alloys. Metall Trans A 24A:481–491

[192] Arnberg L, Backerud L, Klang H (1982) Production and properties of master alloys of AI–Ti–B type and their ability to grain refine aluminium. Metals Technol 9:1–6

[193] Jones GP, Pearson J (1976) Factors affecting the grain-refinement of aluminum using titanium and boron additives. Metall Trans B 7B:223–234

[194] Sigworth GK (1996) Communication on mechanism of grain refinement in aluminum. Scripta Mater 34:919–922

[195] Schumacher P et al (2013) New studies of nucleation mechanisms in aluminium alloys: implications for grain refinement practice. Mater Sci Technol 14(5):394–404. https://doi.org/10.1179/mst.1998.14.5.394

[196] Fan Z (2012) An epitaxial model for heterogeneous nucleation on potent substrates. Metall Mater Trans A 44(3):1409–1418. https://doi.org/10.1007/s11661-012-1495-8

[197] Fan Z et al (2015) Grain refining mechanism in the Al/Al–Ti–B system. Acta Mater 84:292–304. https://doi.org/10.1016/j.actamat.2014.10.055

[198] Lee YC, Dahle AK, StJohn DH (2000) The role of solute in grain refinement of magnesium. Metall Mater Trans A 31A:2895–2906

[199] Men H, Fan Z (2011) Effects of solute content on grain refinement in an isothermal melt. Acta Mater 59(7):2704–2712. https://doi.org/10.1016/j.actamat.2011.01.008

[200] Quested T, Dinsdale A, Greer A (2005) Thermodynamic modelling of growth-restriction effects in aluminium alloys. Acta Mater 53(5):1323–1334. https://doi.org/10.1016/j.actamat.2004.11.024

[201] Schmid-Fetzer R, Kozlov A (2011) Thermodynamic aspects of grain growth restriction in multicomponent alloy solidification. Acta Mater 59(15):6133–6144. https://doi.org/10.1016/j.actamat.2011.06.026

[202] Easton MA, StJohn DH (2001) A model of grain refinement incorporating alloy constitution and potency of heterogenous nucleant particles. Acta Mater 49:1867–1878

[203] Fan Z, Gao F, Zhou L, Lu SZ (2018) A new concept for growth restriction during solidification. Acta Mater 152:248–257. https://doi.org/10.1016/j.actamat.2018.04.045

[204] StJohn DH, Cao P, Qian M, Easton MA (2007) A new analytical approach to reveal the mechanisms of grain refinement. Adv Eng Mater 9(9):739–746. https://doi.org/10.1002/adem.200700157

[205] Easton M, StJohn D (2005) An analysis of the relationship between grain size, solute content and the potency and number density of nucleant particles. Metall Mater Trans 36A:1911–1920

[206] Greer AL, Bunn AM, Tronche A, Evans PV, Bristow DJ (2000) Modelling of inoculation of metallic melts: application to grain refinement of aluminium by Al–Ti–B. Acta Materialia 48(11):2823–2835. https://doi.org/10.1016/S1359-6454(00)00094-X

[207] Günther R, Hartig C, Bormann R (2006) Grain refinement of AZ31 by (SiC)P: theoretical calculation and experiment. Acta Mater 54(20):5591–5597. https://doi.org/10.1016/j.actamat.2006.07.035

[208] Qian M (2007) Heterogeneous nucleation on potent spherical substrates during solidification. Acta Mater

55(3):943–953. https://doi.org/10.1016/j.actamat.2006.09.016

[209] Qian M et al (2010) An analytical model for constitutional supercooling-driven grain formation and grain size prediction. Acta Mater 58(9):3262–3270. https://doi.org/10.1016/j.actamat.2010.01.052

[210] Turnbull D, Vonnegut B (1952) Nucleation Catalysis. Ind Eng Chem 44(6):1292–1298. https://doi.org/10.1021/ie50510a031

[211] Liu S et al (2009) Effect of Mg–TiB_2 master alloy on the grain refinement of AZ91D magnesium alloy. J Alloy Compd 487(1–2):202–205. https://doi.org/10.1016/j.jallcom.2009.08.065

[212] Wang Y et al (2011) Characterisation of magnesium oxide and its interface with α-Mg in Mg–Al-based alloys. Philos Mag Lett 91(8):516–529. https://doi.org/10.1080/09500839.2011.591744

[213] Zhang MX, Kelly PM (1999) Edge to edge matching—a new approach to the morphology and crystallography of precipitates. Mater Forum 23:22

[214] Zhang MX, Kelly PM (2005) Edge-to-edge matching and its applications. Acta Mater 53(4):1085–1096. https://doi.org/10.1016/j.actamat.2004.11.005

[215] Zhang MX, Kelly PM (2005) Edge-to-edge matching and its applications. Acta Mater 53(4):1073–1084. https://doi.org/10.1016/j.actamat.2004.11.007

[216] Qiu D et al (2009) A new approach to designing a grain refiner for Mg casting alloys and its use in Mg–Y-based alloys. Acta Mater 57(10):3052–3059. https://doi.org/10.1016/j.actamat.2009.03.011

[217] Wang F et al (2016) A refining mechanism of primary Al_3Ti intermetallic particles by ultrasonic treatment in the liquid state. Acta Mater 116:354–363. https://doi.org/10.1016/j.actamat.2016.06.056

[218] Liu Z et al (2014) The grain refining mechanism of cast zinc through silver inoculation. Acta Mater 79:315–326. https://doi.org/10.1016/j.actamat.2014.07.026

[219] Kelly PM, Zhang MZ (2006) Edge to edge matching—the fundamentals. Metall Mater Trans A 37A:833–839

[220] Zhang MX, Kelly PM (2005) Edge-to-edge matching model for predicting orientation relationships and habit planes—the improvements. Scripta Mater 52(10):963–968. https://doi.org/10.1016/j.scriptamat.2005.01.040